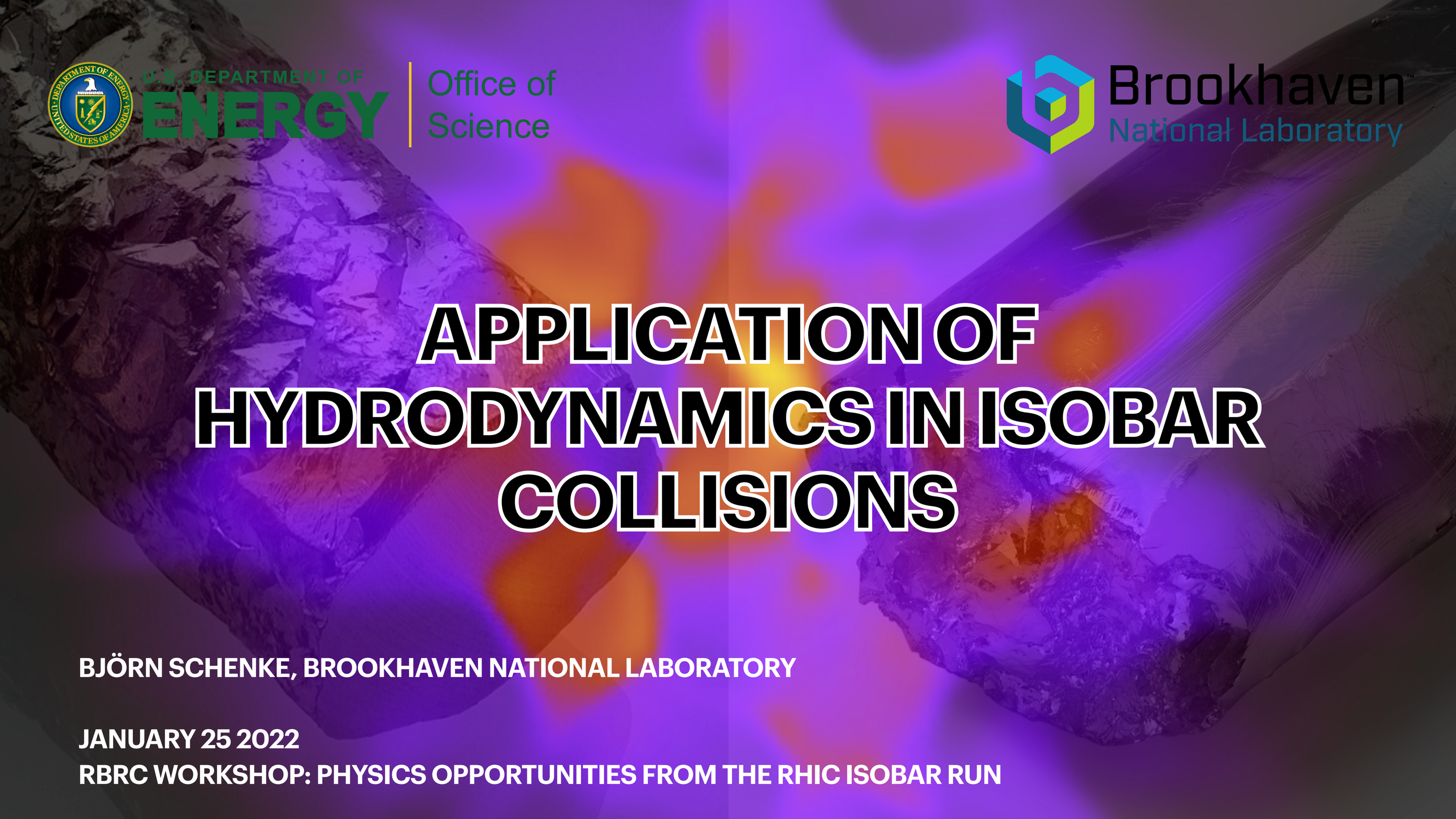

U.S. DEPARTMENT OF ENERGY | Office of Science

Brookhaven National Laboratory

APPLICATION OF HYDRODYNAMICS IN ISOBAR COLLISIONS

BJÖRN SCHENKE, BROOKHAVEN NATIONAL LABORATORY

JANUARY 25 2022

RBRC WORKSHOP: PHYSICS OPPORTUNITIES FROM THE RHIC ISOBAR RUN

Produced particles know about the geometry of the collision

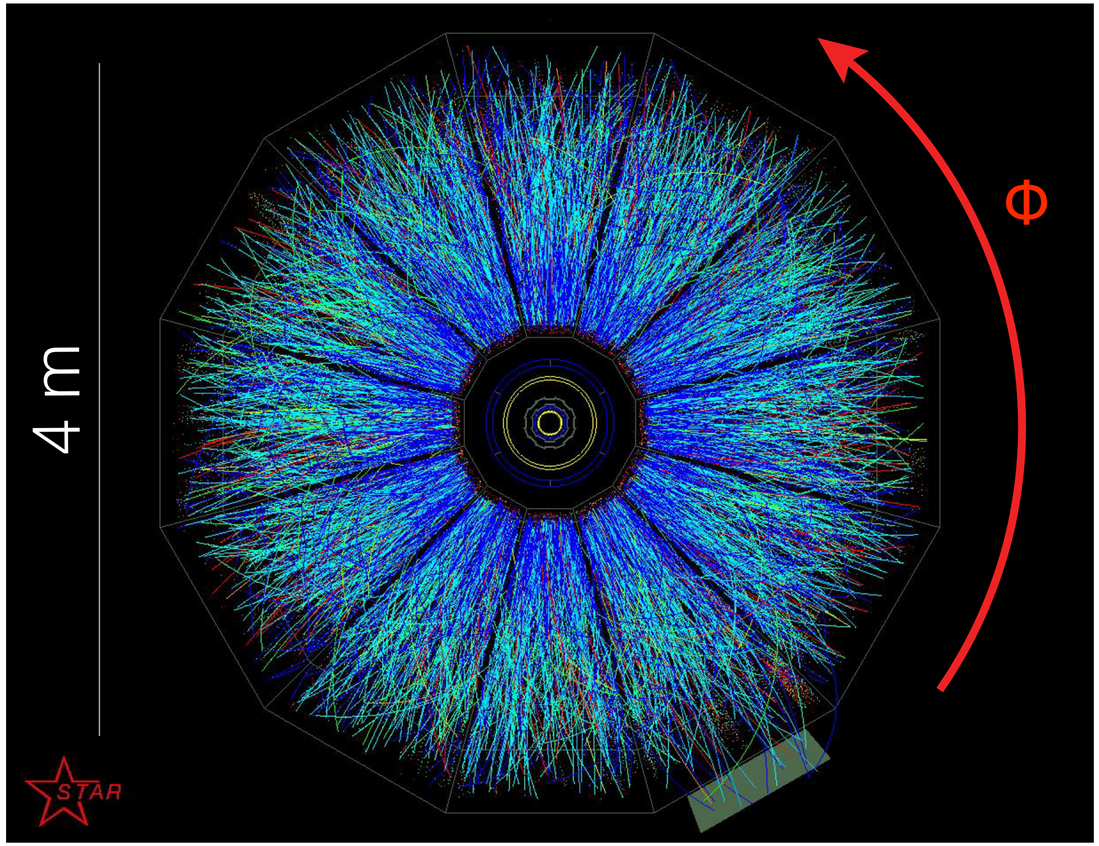

Azimuthal anisotropies in particle spectra

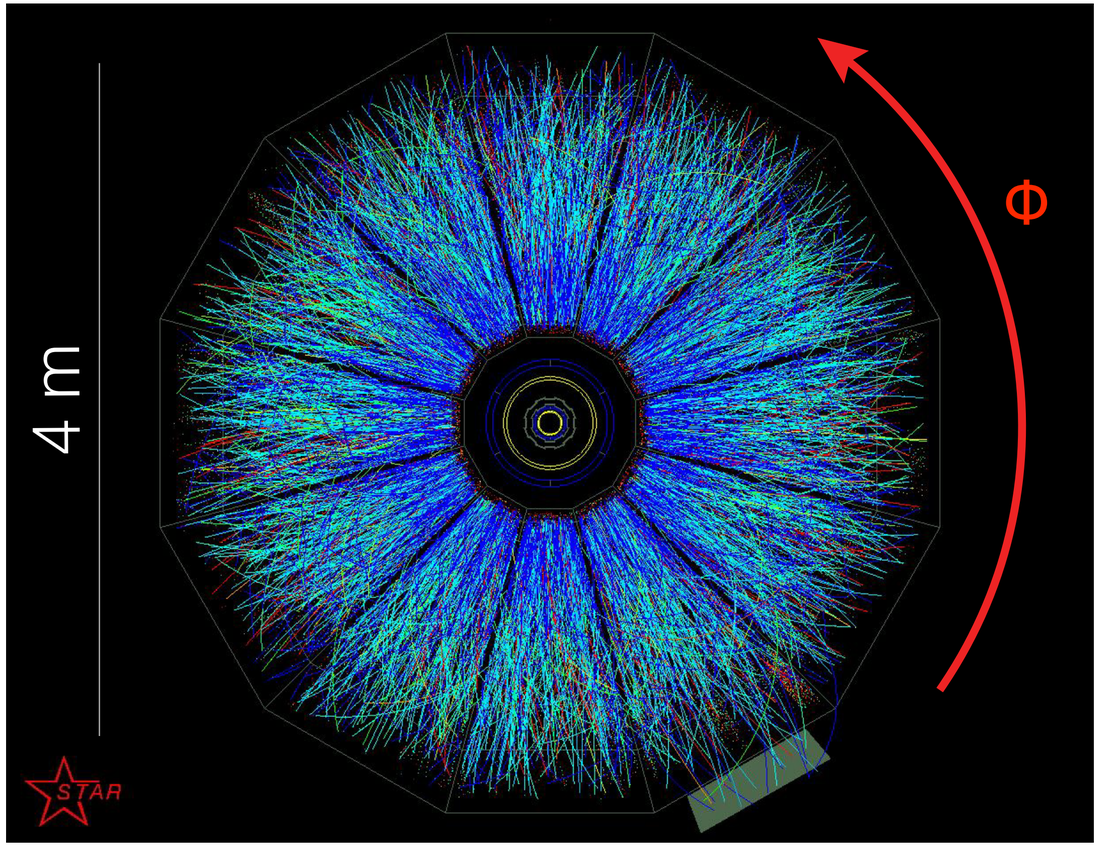

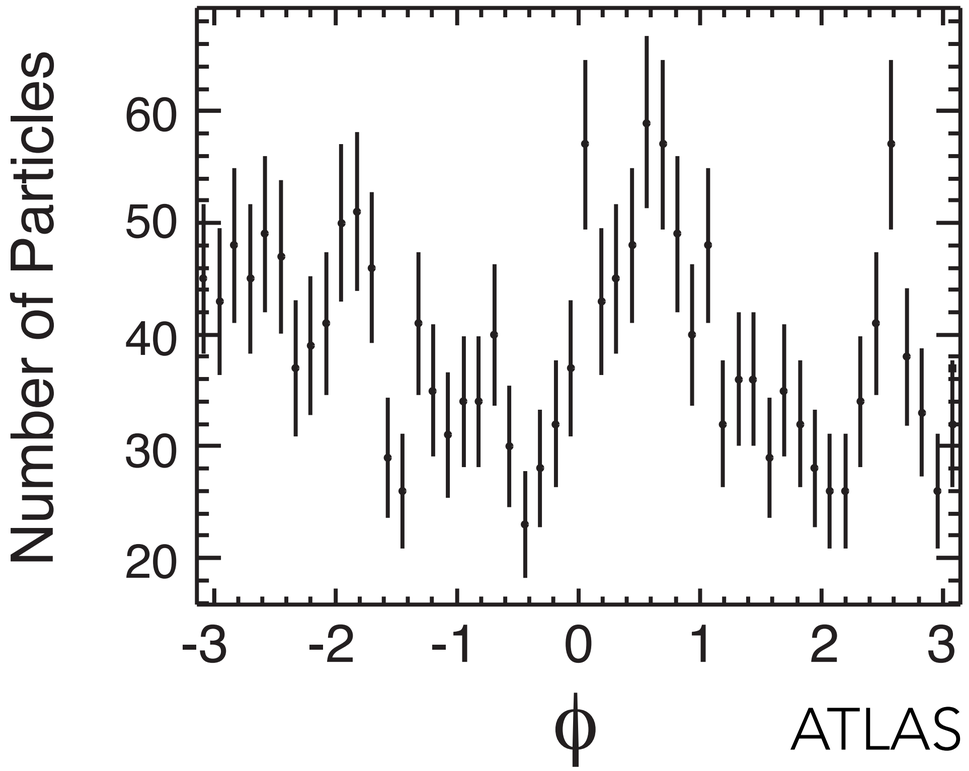

Azimuthal anisotropies in particle spectra

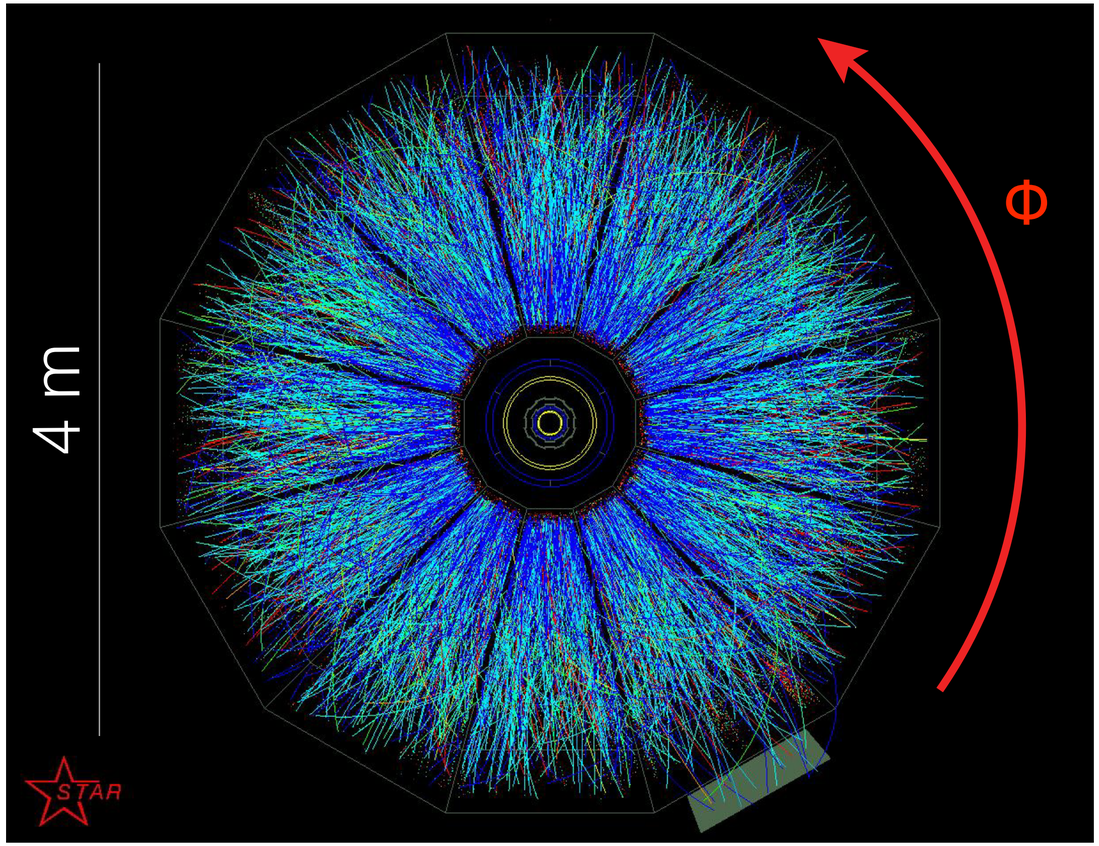

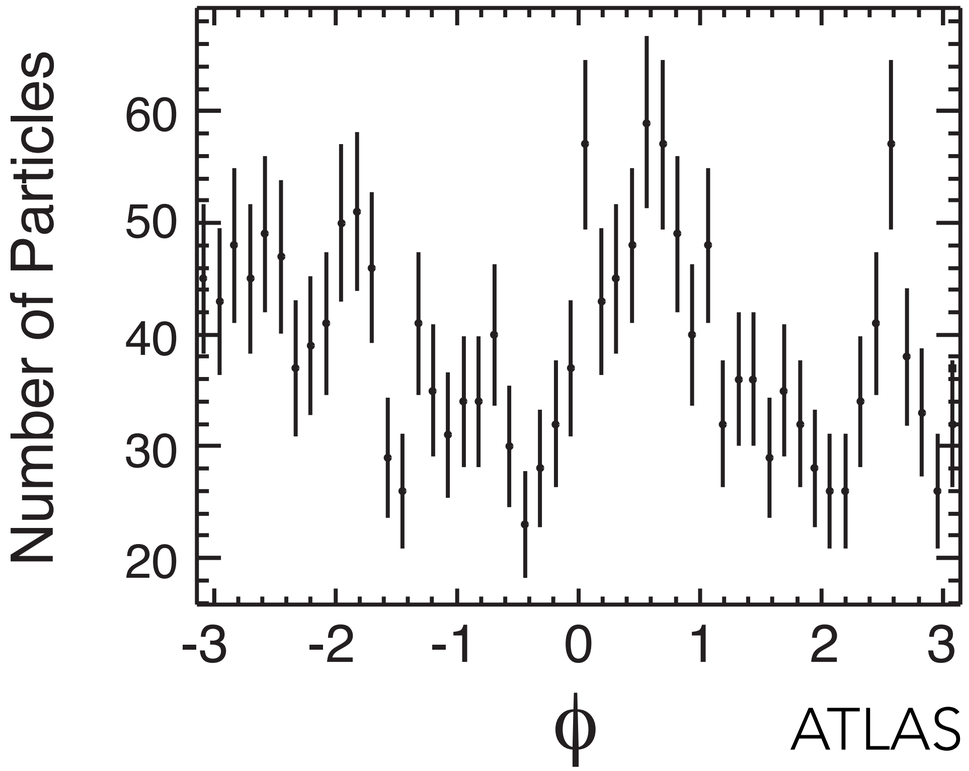

Quantify anisotropy using Fourier expansion: $\frac{dN}{d\phi} = \frac{N}{2\pi}\left(1 + \sum_n 2v_n \cos[n(\phi - \psi_n)]\right)$

Azimuthal anisotropies in particle spectra

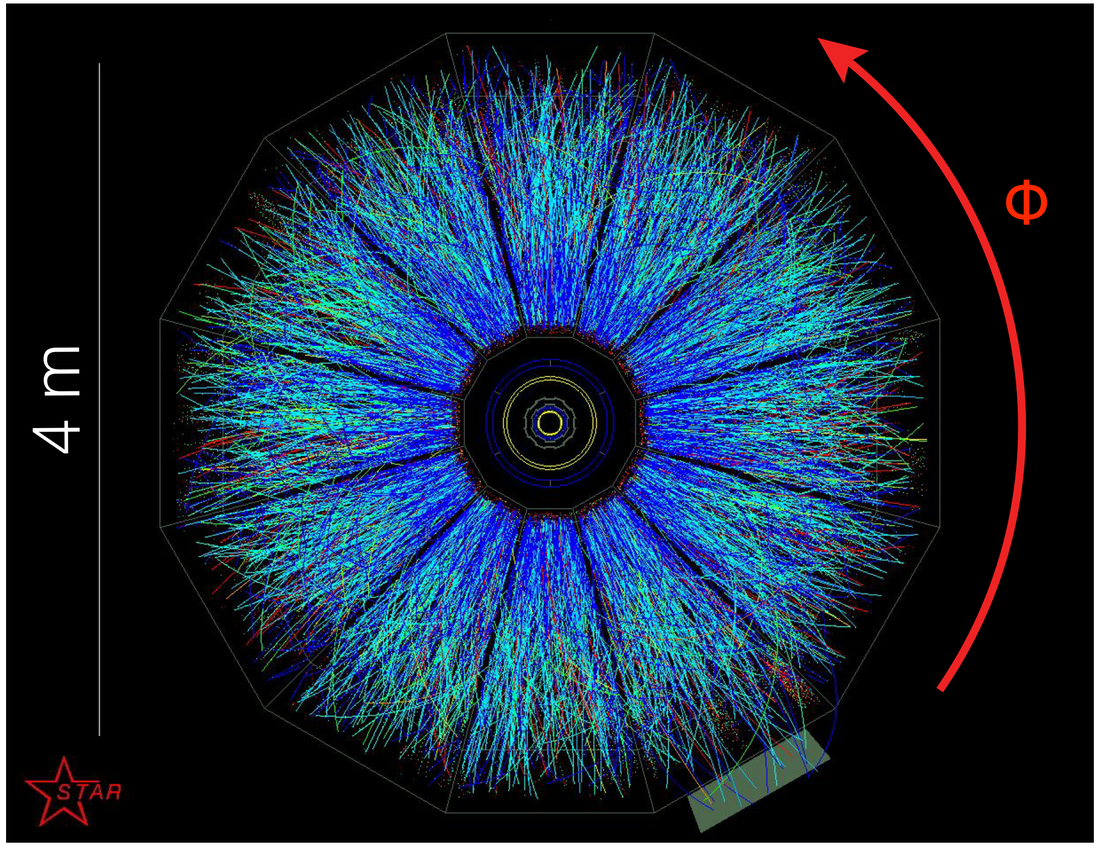

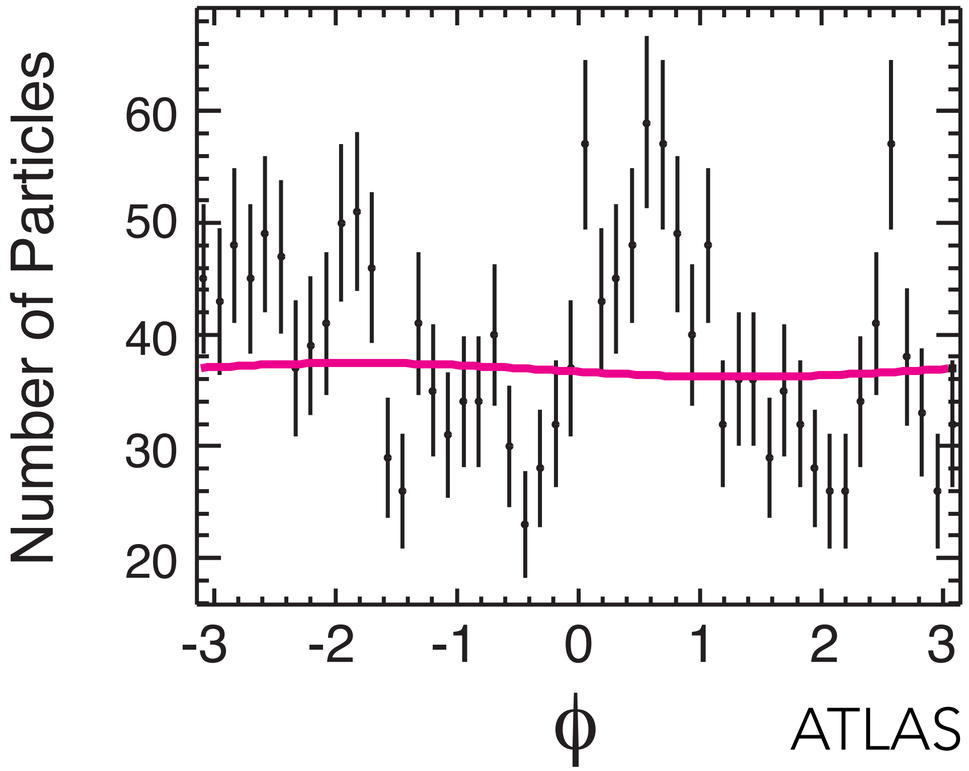

$$\frac{dN}{d\phi} = \frac{N}{\pi}\left(\frac{1}{2} + v_1 \cos[(\phi - \psi_1)]\right)$$

Azimuthal anisotropies in particle spectra

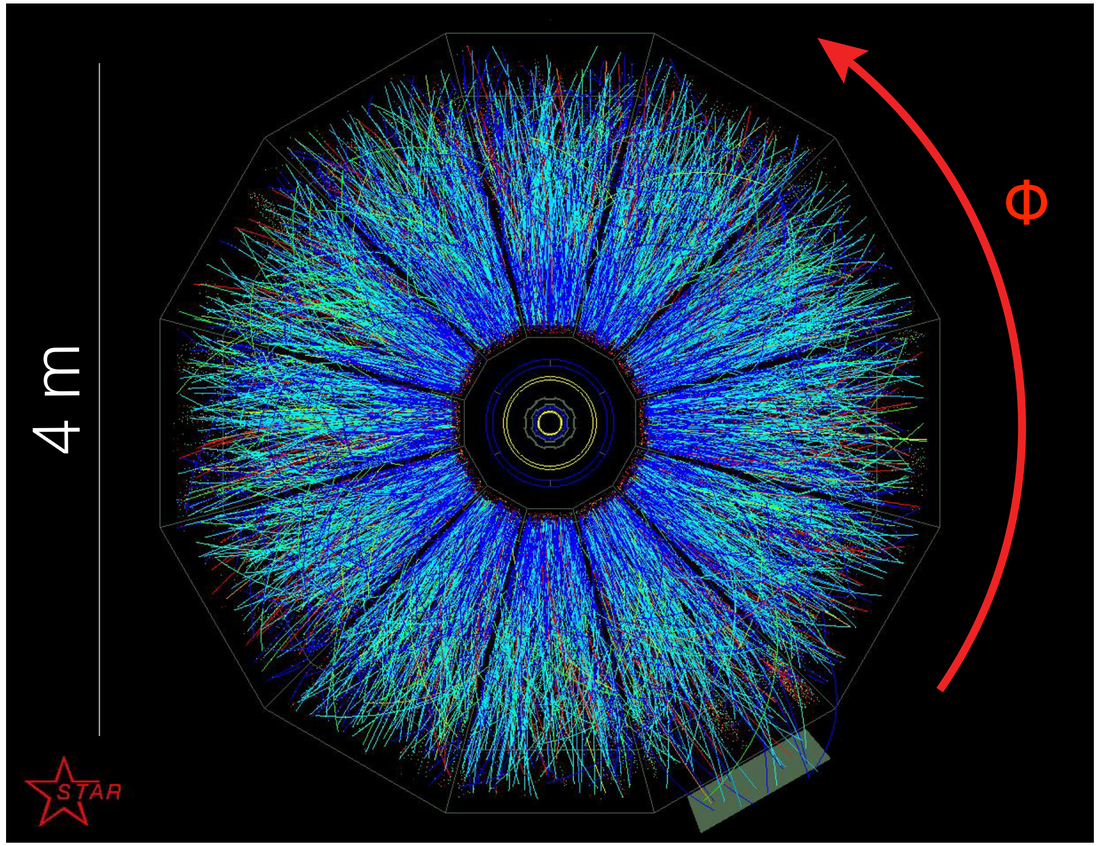

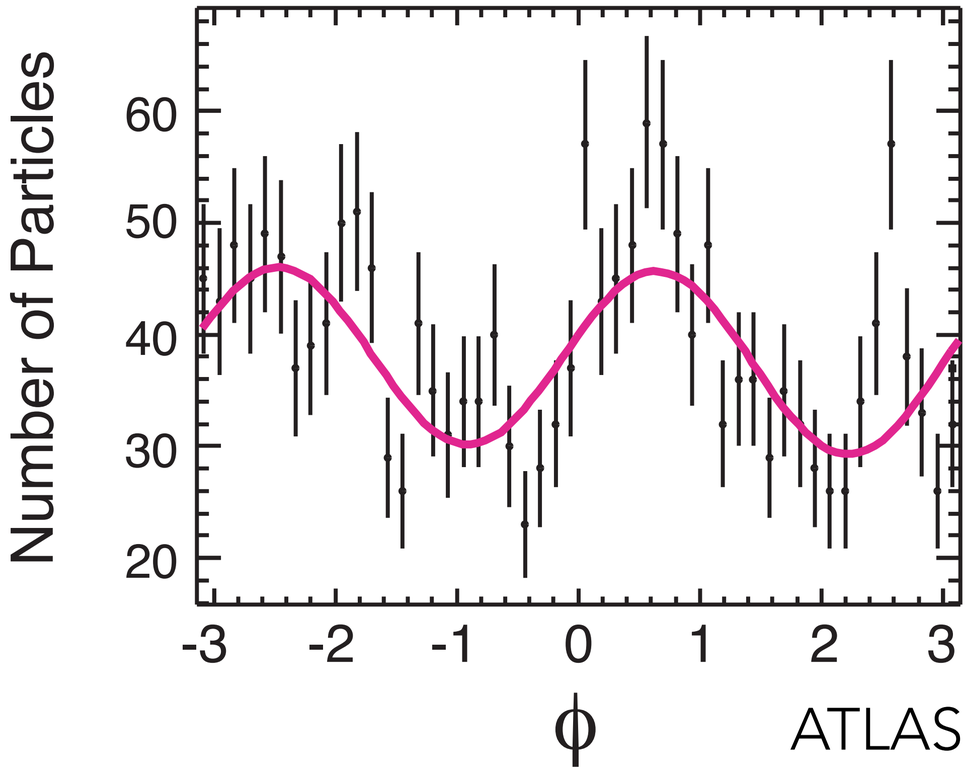

$$\frac{dN}{d\phi} = \frac{N}{\pi}\left(\frac{1}{2} + v_1 \cos[(\phi - \psi_1)] + v_2 \cos[2(\phi - \psi_2)]\right)$$

Azimuthal anisotropies in particle spectra

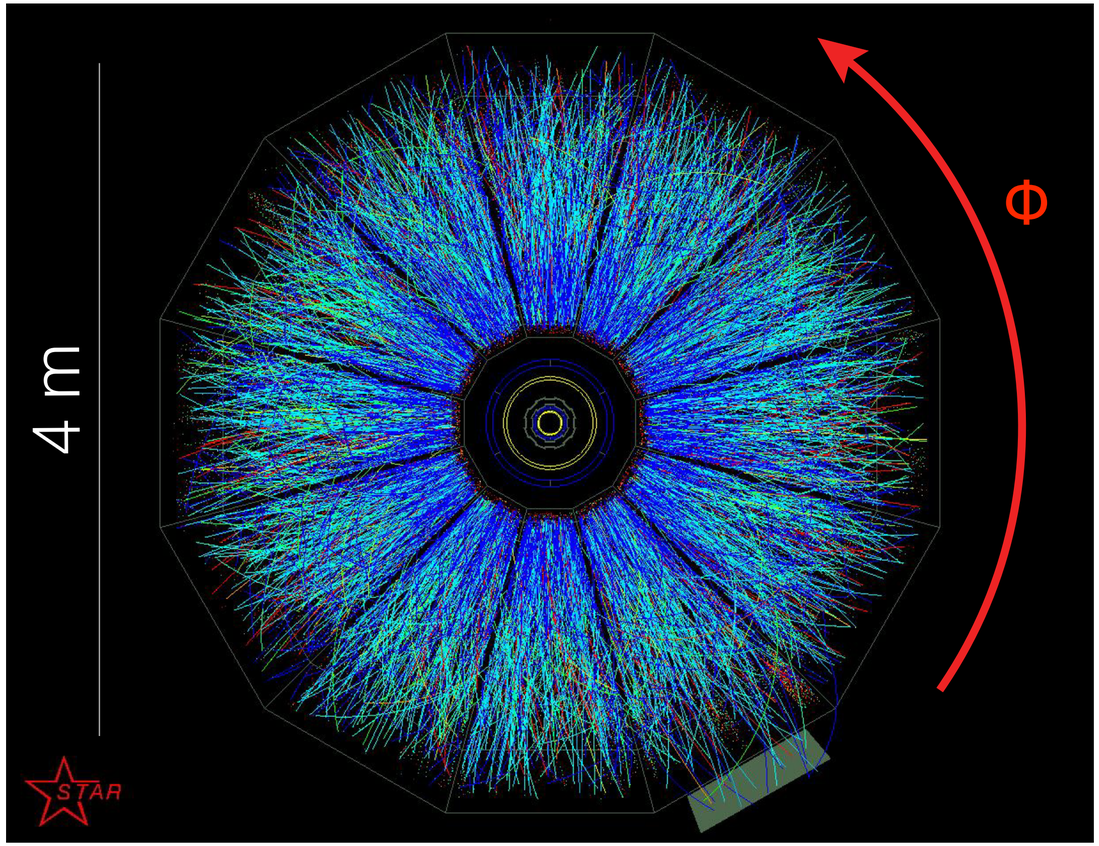

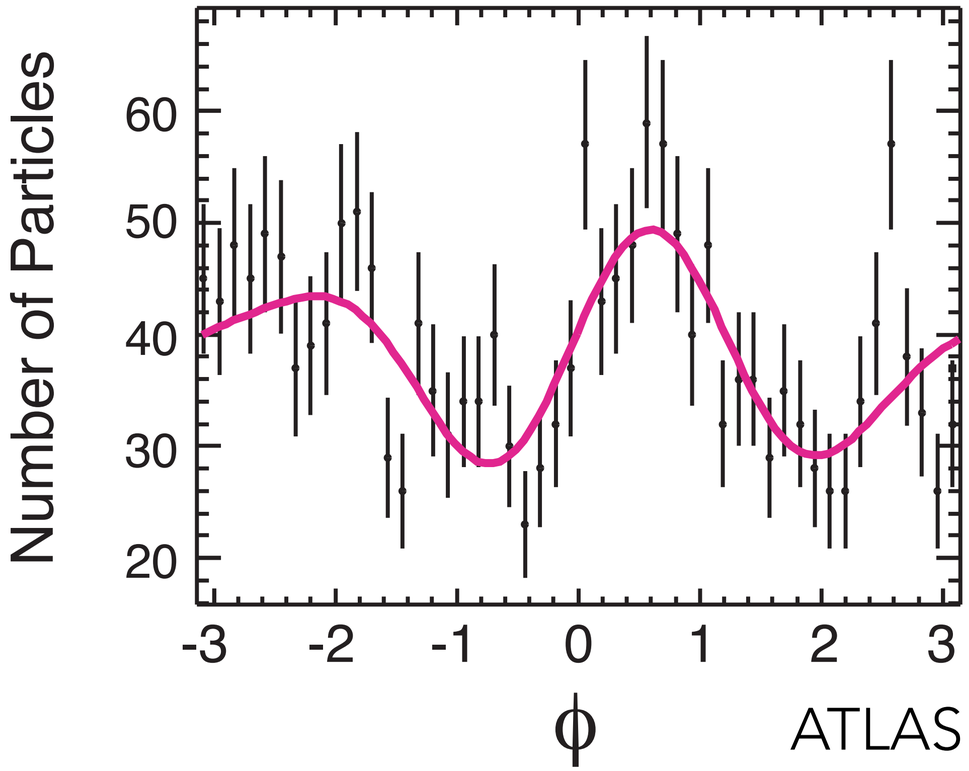

$$\frac{dN}{d\phi} = \frac{N}{\pi}\left(\frac{1}{2} + v_1 \cos[(\phi - \psi_1)] + v_2 \cos[2(\phi - \psi_2)] + v_3 \cos[3(\phi - \psi_3)]\right)$$

Azimuthal anisotropies in particle spectra

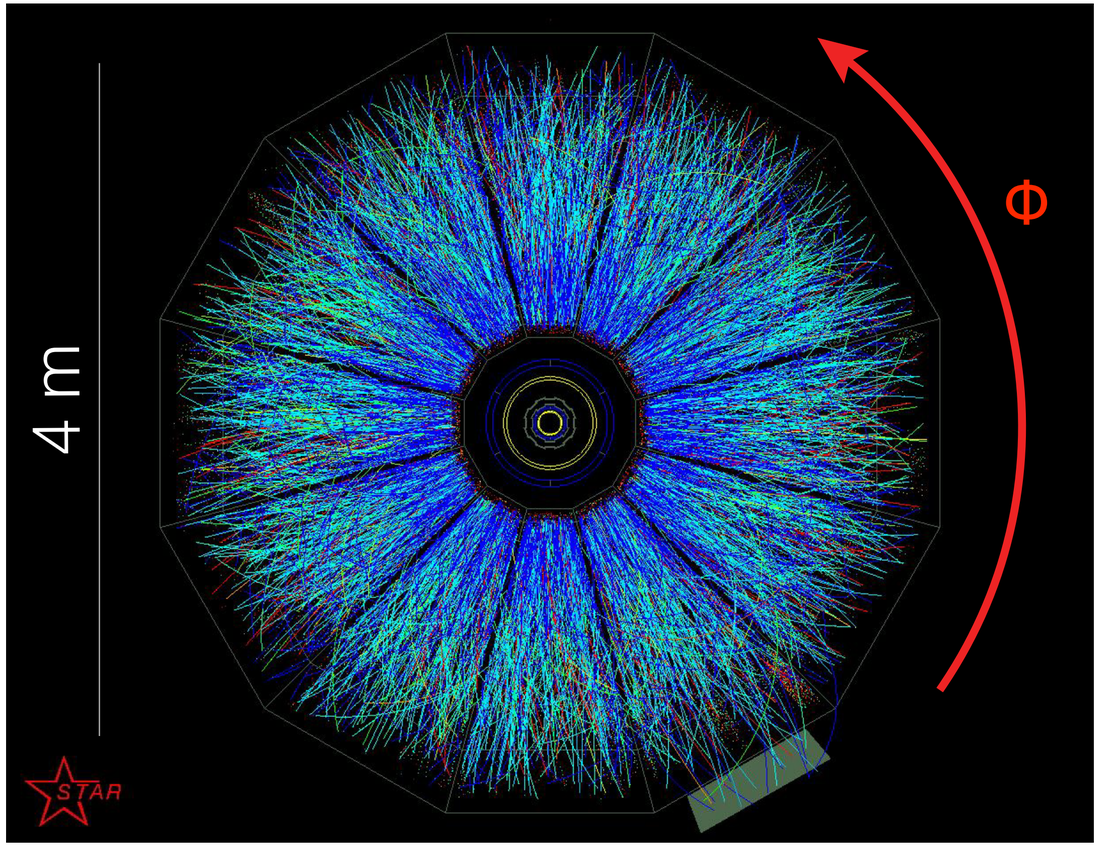

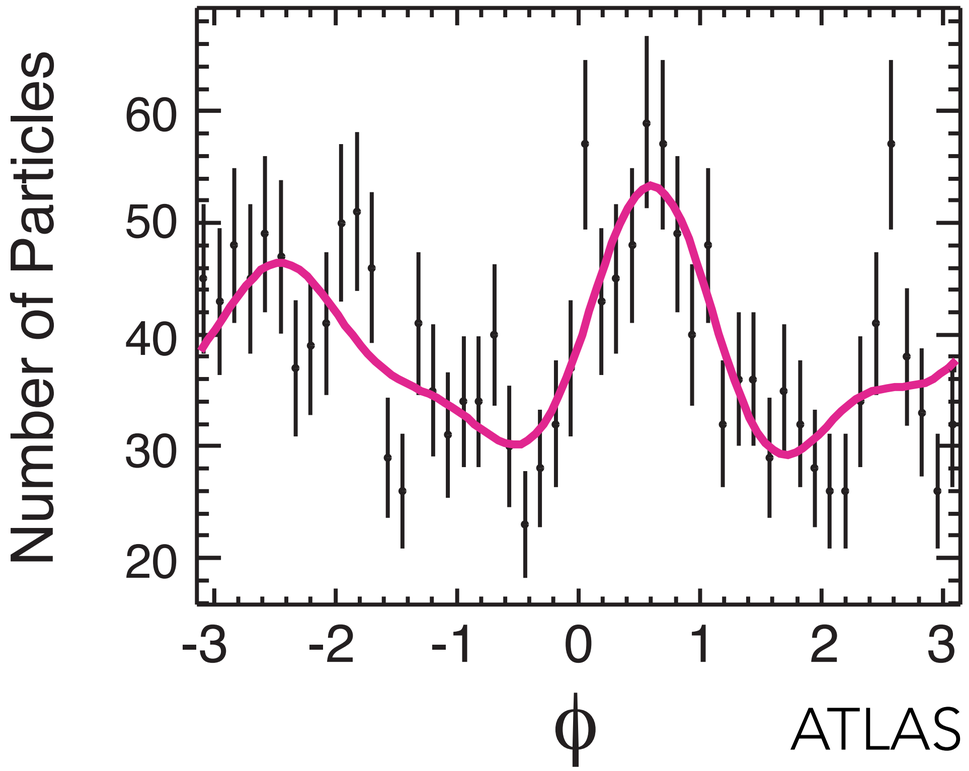

$$\frac{dN}{d\phi} = \frac{N}{\pi}\left(\frac{1}{2} + v_1 \cos[(\phi - \psi_1)] + v_2 \cos[2(\phi - \psi_2)] + v_3 \cos[3(\phi - \psi_3)] + v_4 \cos[4(\phi - \psi_4)]\right)$$

Azimuthal anisotropies in particle spectra

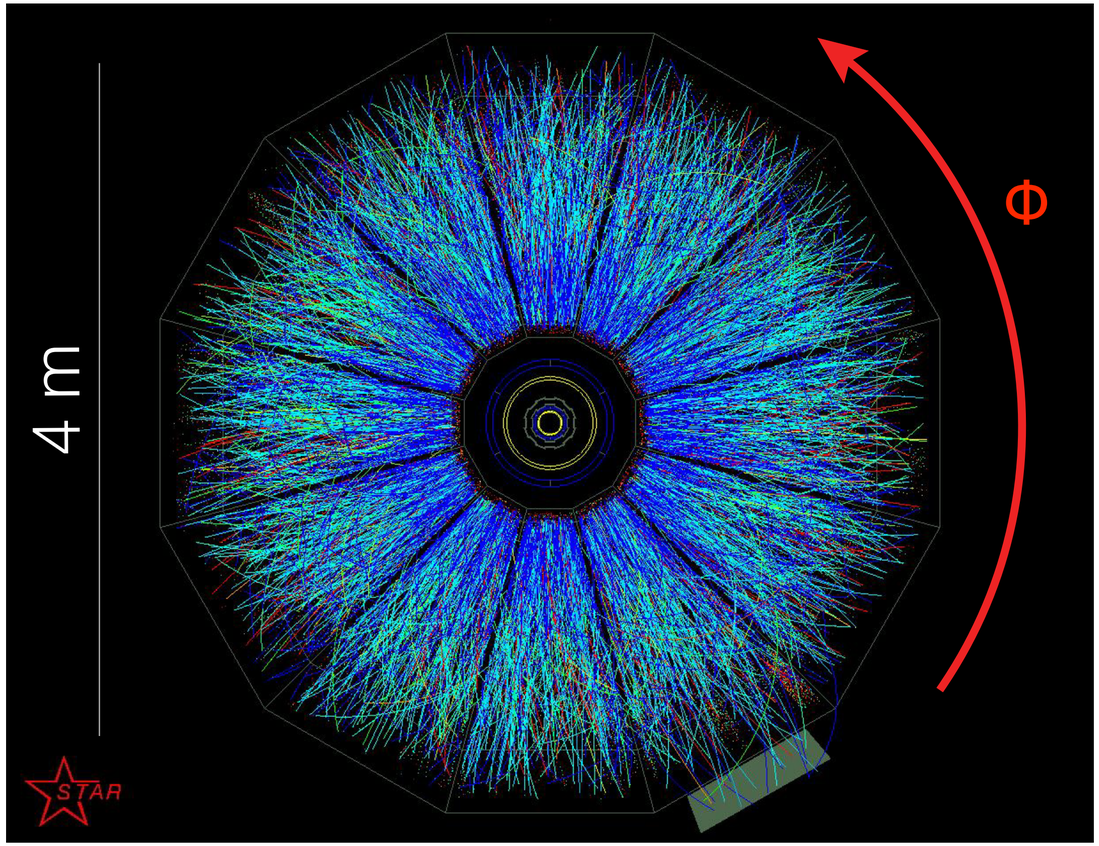

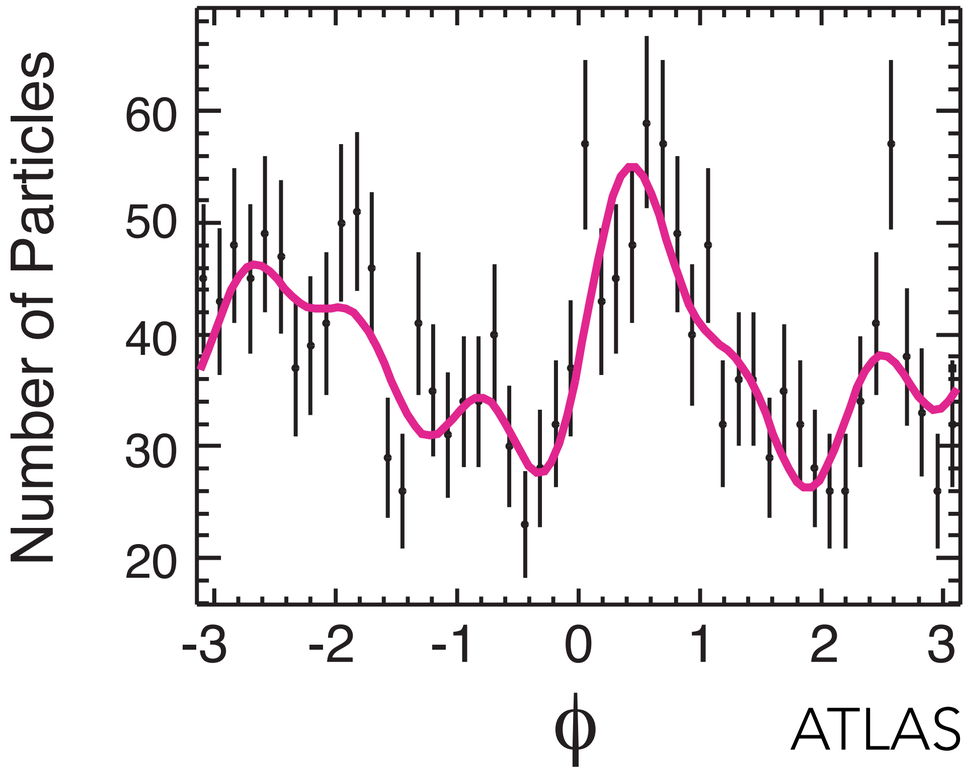

$$\frac{dN}{d\phi} = \frac{N}{\pi}\left(\frac{1}{2} + v_1 \cos[(\phi - \psi_1)] + v_2 \cos[2(\phi - \psi_2)] + v_3 \cos[3(\phi - \psi_3)] + v_4 \cos[4(\phi - \psi_4)] + \ldots\right)$$

In practice: use multi-particle correlations

2-particle correlation vs. Δη and Δϕ:

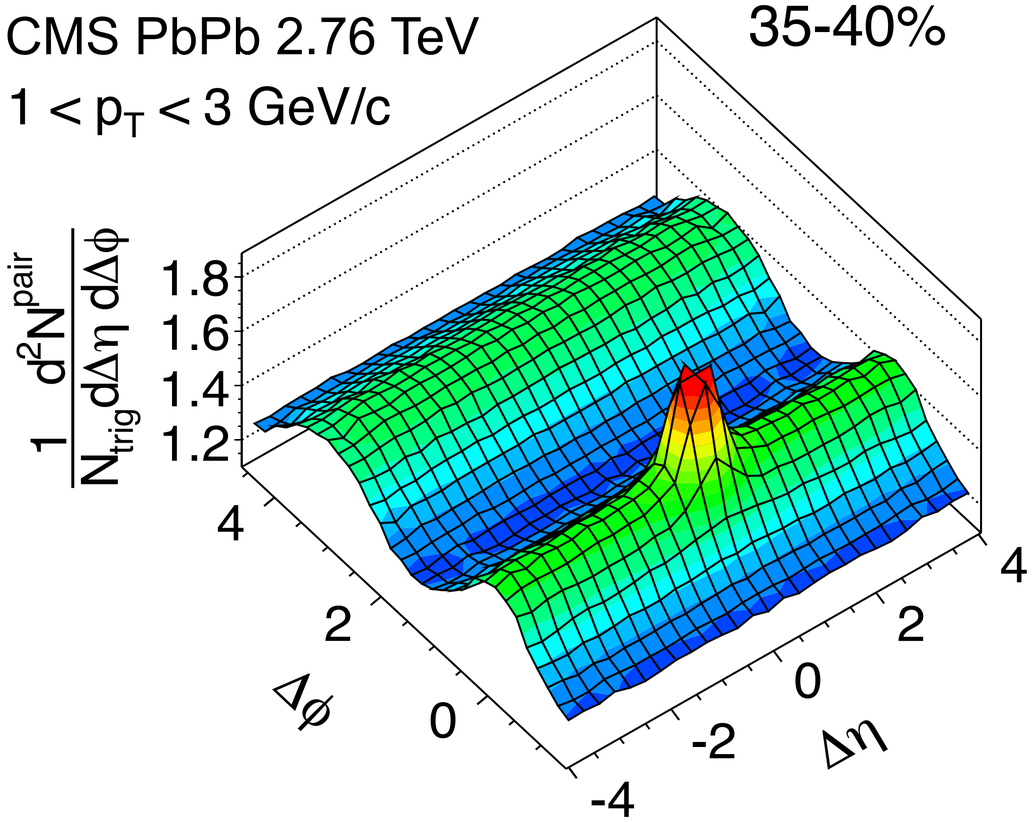

CMS COLL., EUR. PHYS. J. C72 (2012)

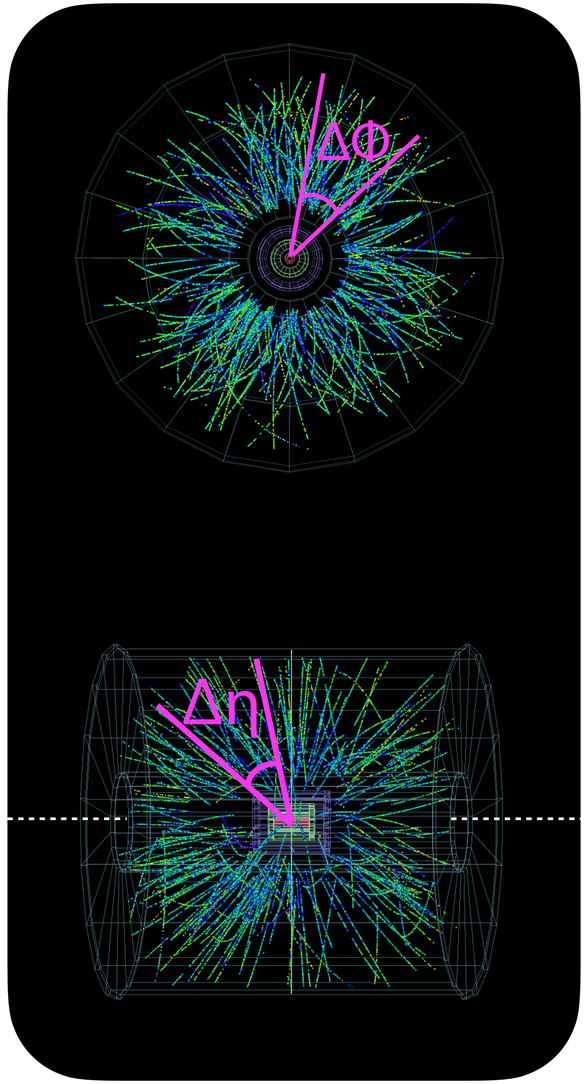

Event Displays: © 2012 CERN, ALICE

ΔΦ: DIFFERENCE IN AZIMUTHAL ANGLE

Δη: DIFFERENCE IN PSEUDO-RAPIDITY

Long known: Elliptic flow (v_2) sensitive to initial shape

STAR Collaboration, Phys.Rev.Lett. 86 (2001) 402-407

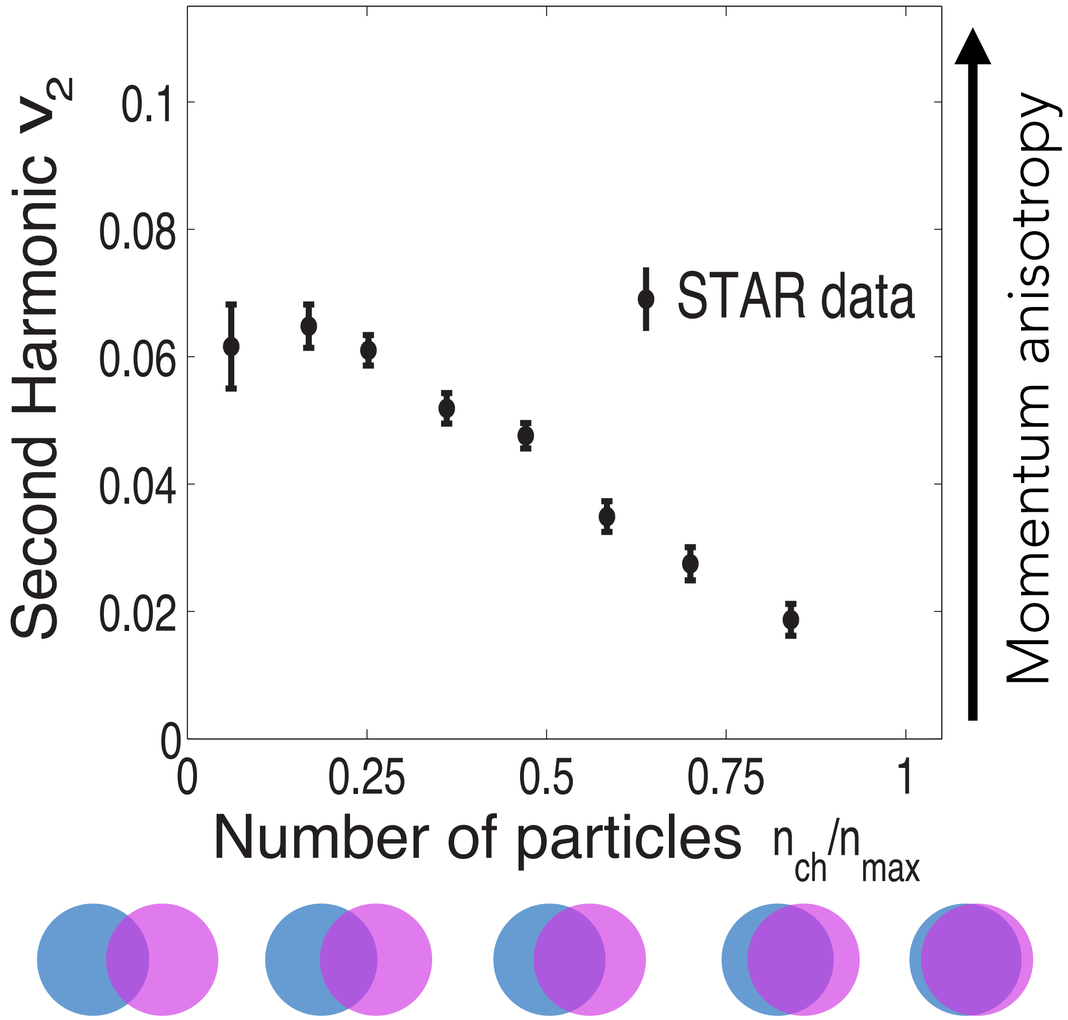

Experimentally found correlation between initial shape and momentum anisotropy

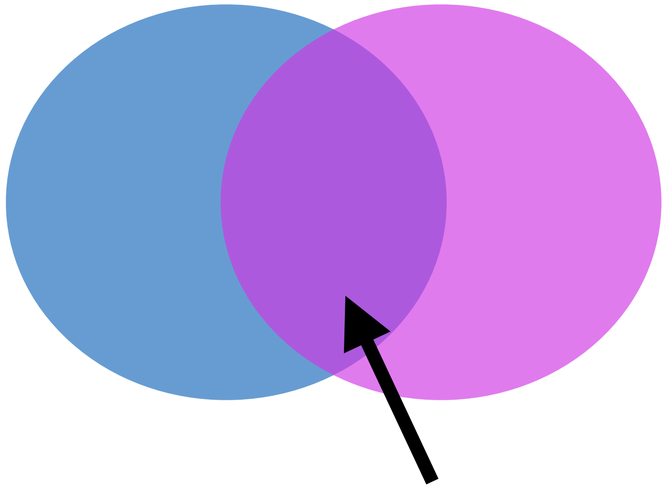

~ elliptic interaction region

Interpretation: Strong final state effects

Azimuthal momentum anisotropy generated by medium response to the initial transverse geometry: Pressure gradients drive expansion

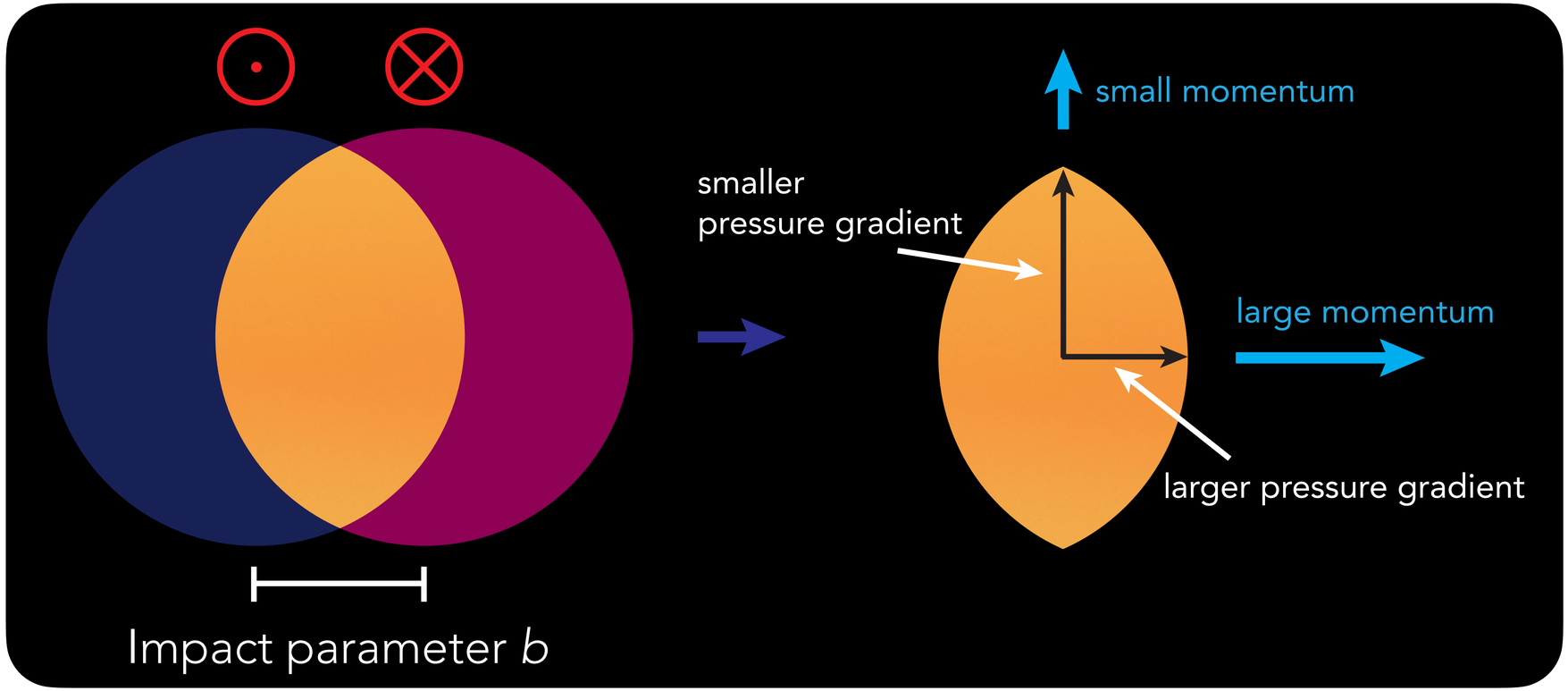

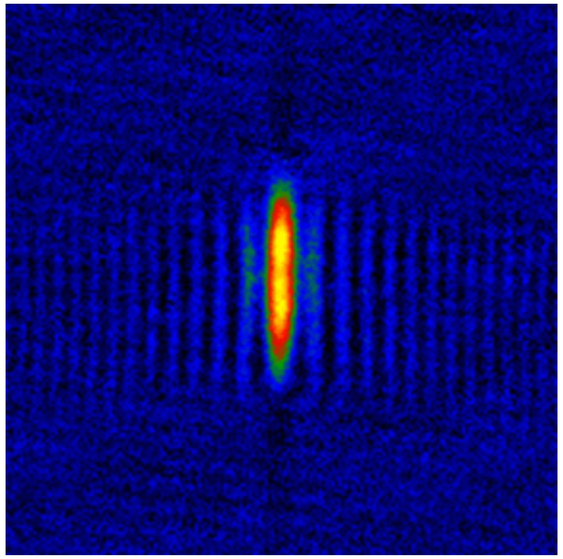

"A cigar-shaped cloud of fermionic ^{6}Li atoms is confined and rapidly cooled to degeneracy in a CO_2 laser trap [...] Upon abruptly turning off the trap, t he gas exhibits a spectacular anisotropic expansion."
K. M. O'Hara et al., Science Volume 298, pp. 2179-2182 (2002)

Interpretation: Strong final state effects

Generally, fluctuating structure generates all moments

Reason: Nucleon- and sub-nucleon degrees of freedom

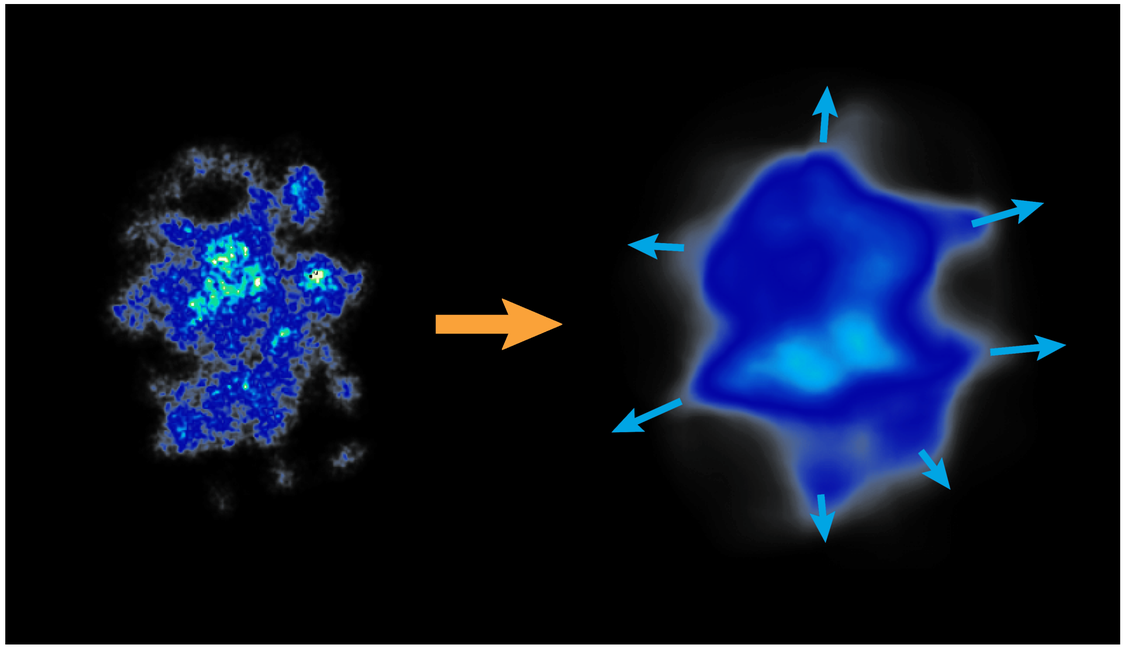

Initial energy density distribution

Hydrodynamic expansion

Fourier components of initial geometry

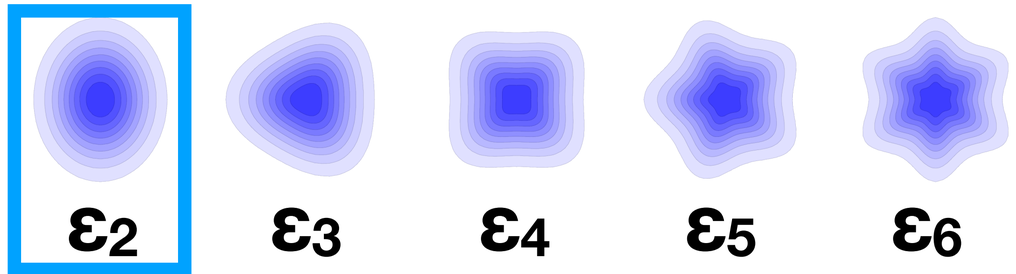

$\varepsilon_n \sim v_n$

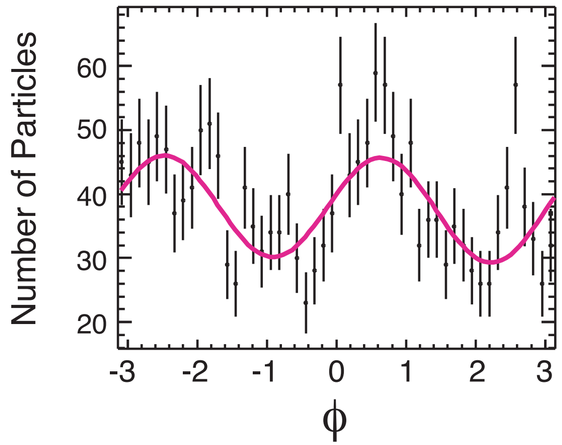

Analogously, mean transverse momentum ~ 1/radius

At fixed multiplicity, a smaller size means larger pressure gradients, which means larger mean transverse momentum $\langle p_T \rangle$

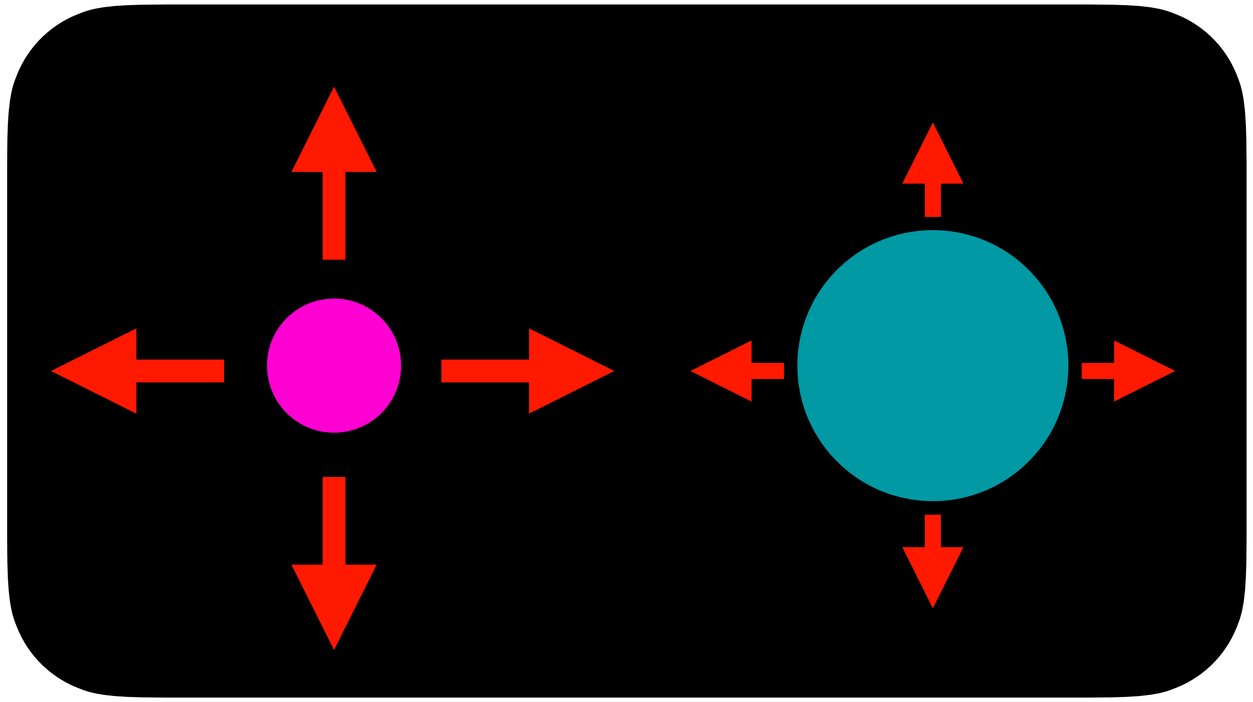

Giacalone et al., Phys. Rev. C 103 (2021) 024909

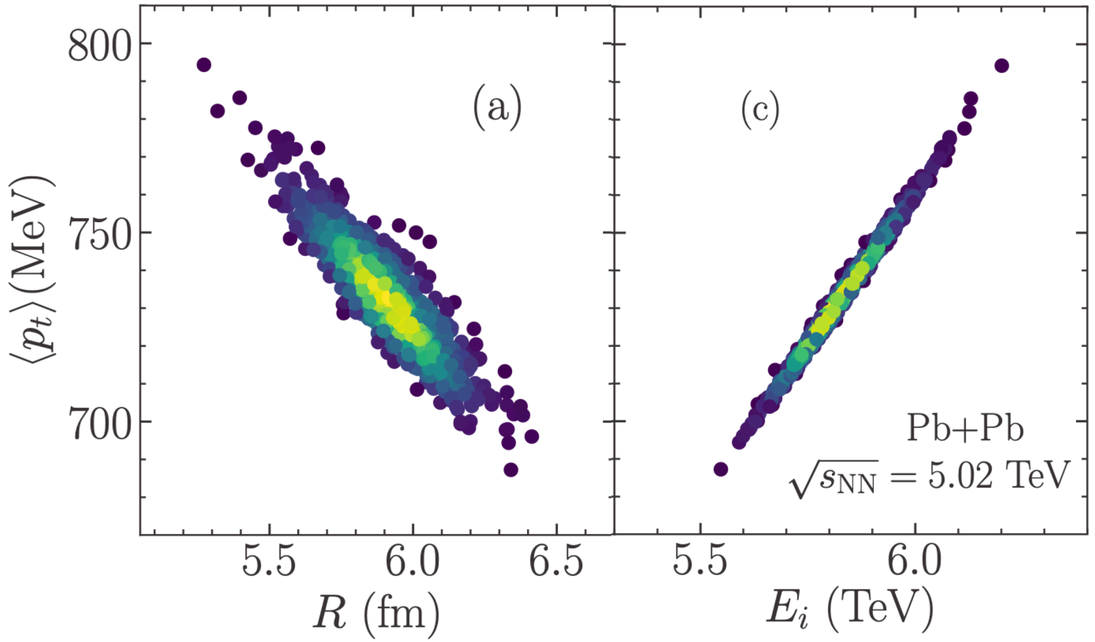

~same total initial entropy

Analogously, mean transverse momentum ~ 1/radius

At fixed multiplicity, a smaller size means larger pressure gradients, which means larger mean transverse momentum $\langle p_T \rangle$

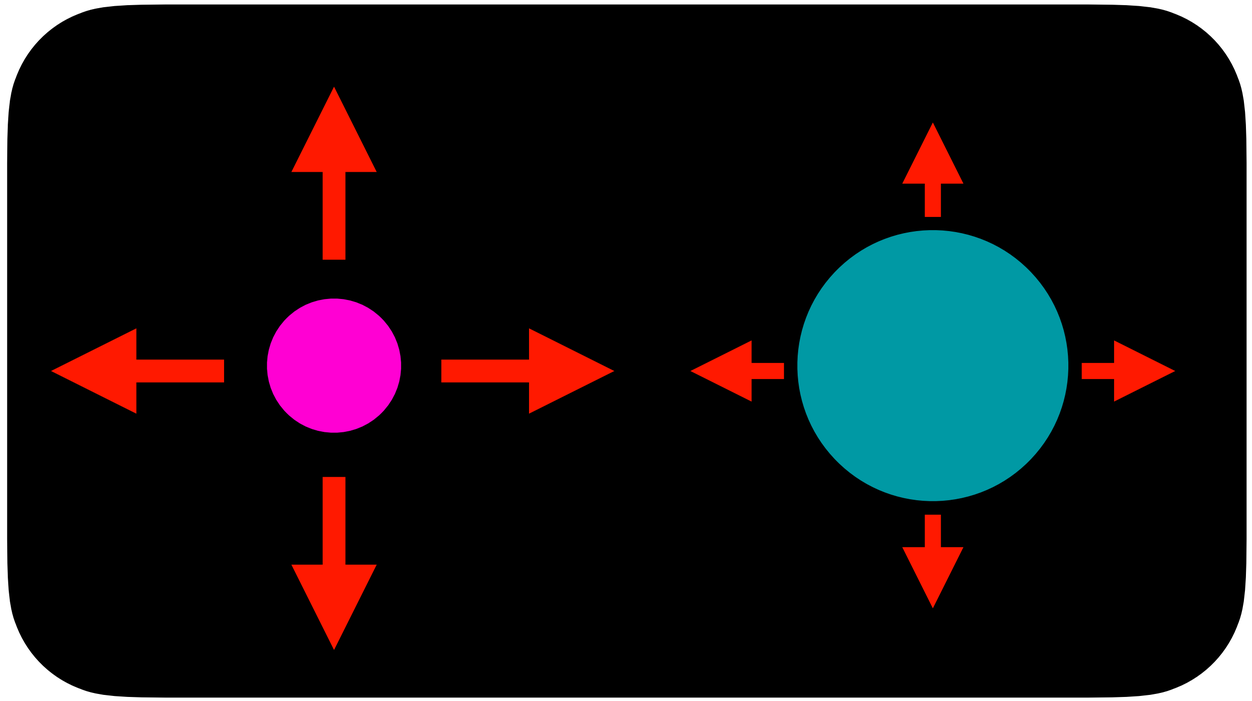

Schenke, Shen, Teaney, *Phys.Rev.C* 102 (2020) 3, 034905

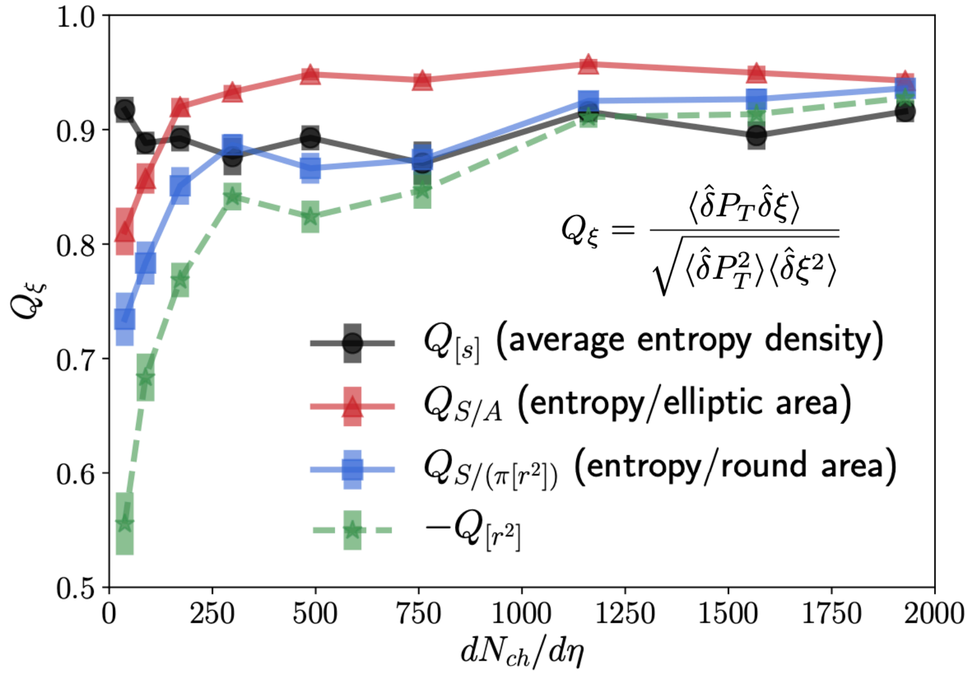

~same total initial entropy

Relativistic fluid dynamics

- Effective theory for the long wavelength modes, valid for a strongly interacting system

- Basic equations: **energy and momentum conservation**

energy density pressure

$$\partial_\mu T^{\mu\nu} = 0 \quad \text{with} \quad T^{\mu\nu} = (\varepsilon + P) u^\mu u^\nu - P g^{\mu\nu} + \Pi^{\mu\nu}$$

flow velocity viscous correction

- + constituent equations for $\Pi^{\mu\nu}$

  (contains shear viscosity η and bulk viscosity ζ, possibly heat conductivity and higher order transport coefficients)

- Equation of state $P(\varepsilon)$ relates pressure to energy density (from lattice QCD)

Conversion is more effective for more ideal fluids

$\eta/s = 0$

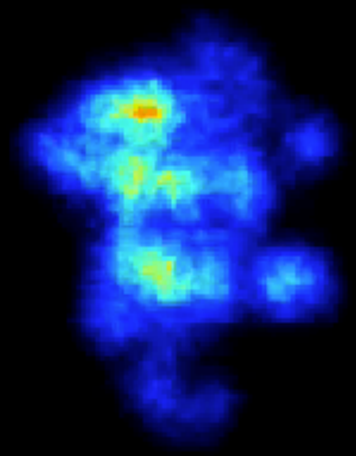

$\eta/s = 0.1$

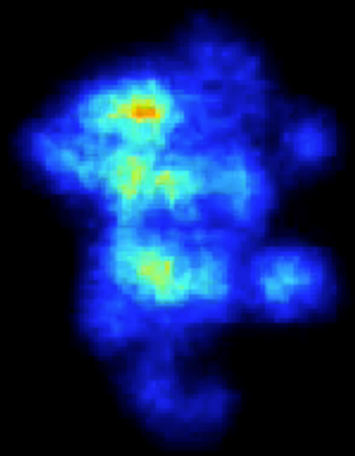

$\eta/s = 0.2$

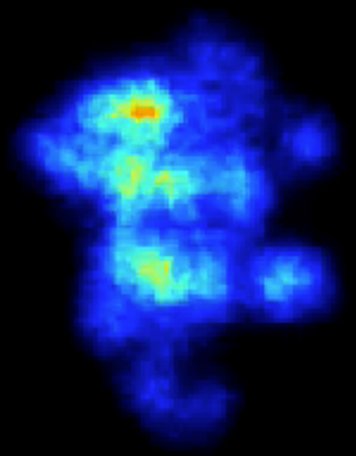

MUSIC hydrodynamic simulation

t = 0.40 fm

B. Schenke, S. Jeon, C. Gale, Phys. Rev. C82, 014903 (2010); Phys. Rev. Lett. 106, 04230 (2011)

Nuclear shape will matter

Shape of colliding nuclei 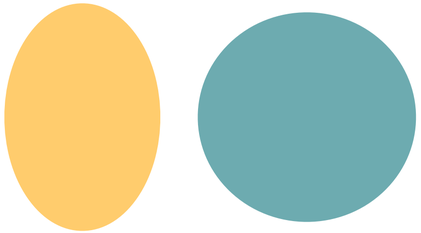 affects shape of interaction regions

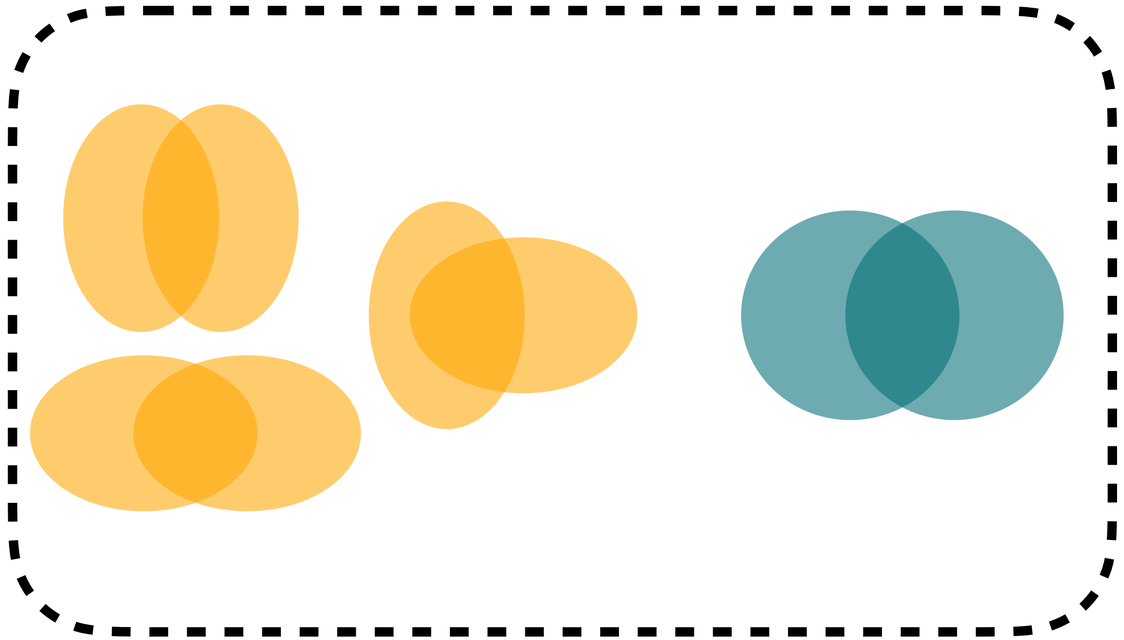

(more so in very central events)

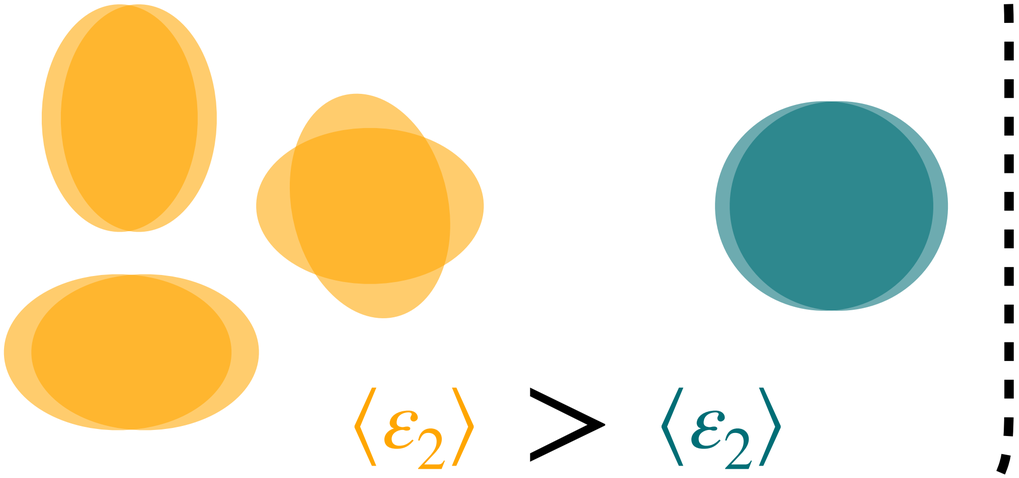

which affects final particle distribution

Isobars: Expectations from a Monte-Carlo Glauber model

Motivation for the isobar run: Expected almost identical geometries for the two isobars ${}^{96}_{44}Ru$ and ${}^{96}_{40}Zr$, yielding ~identical backgrounds for the CME **Deng et al., *Phys.Rev.C* 94 (2016) 041901**

Use a Monte-Carlo Glauber model; nucleon positions sampled from a Woods-Saxon distribution

$$\rho(r,\theta) = \frac{\rho_0}{1+\exp[(r-R'(\theta))/a]}$$

with $R'(\theta) = R[1+\beta_2 Y_2^0(\theta)+\beta_3 Y_3^0(\theta)+\beta_4 Y_4^0(\theta)]$

ρ_0: nuclear density at the center of the nucleus
$Y_l^m(\theta)$: spherical harmonics
$\beta_2, \beta_3, \beta_4$: deformation parameters
a: skin depth

Often one assumes the same distribution for protons and neutrons. Long known not to be true [Chaumeaux et al., Annals. Phys. 116, 247 (1978)]

Expectations from a Monte-Carlo Glauber model

In **Deng et al., *Phys.Rev.C* 94 (2016) 041901** they used

Ru: $R = 5.085\,\mathrm{fm}$; $a = 0.46\,\mathrm{fm}$; $\beta_2 = 0.158$ (case 1) $\beta_2 = 0.053$ (case 2); $\beta_3 = 0$; $\beta_4 = 0$

Zr: $R = 5.02\,\mathrm{fm}$; $a = 0.46\,\mathrm{fm}$; $\beta_2 = 0.08$ (case 1) $\beta_2 = 0.217$ (case 2); $\beta_3 = 0$; $\beta_4 = 0$

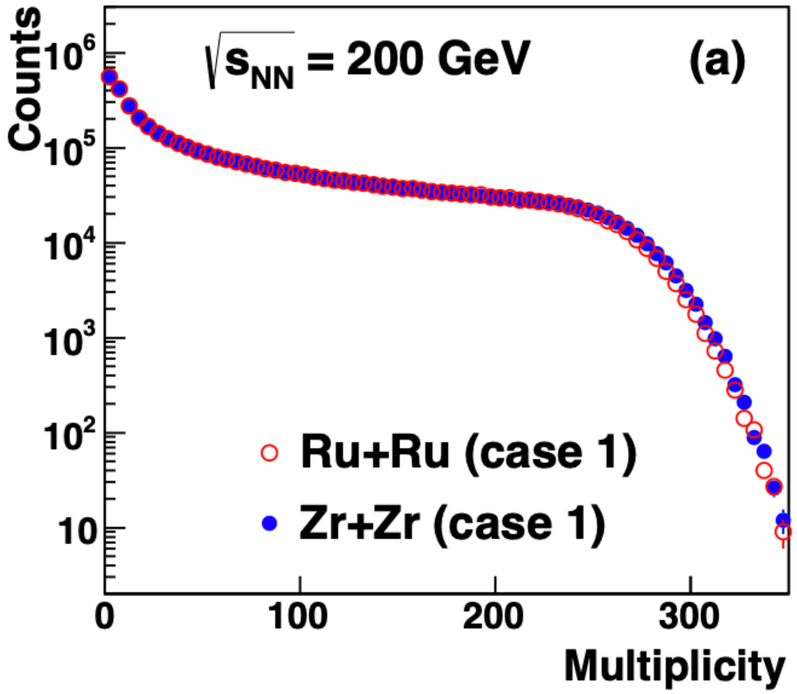

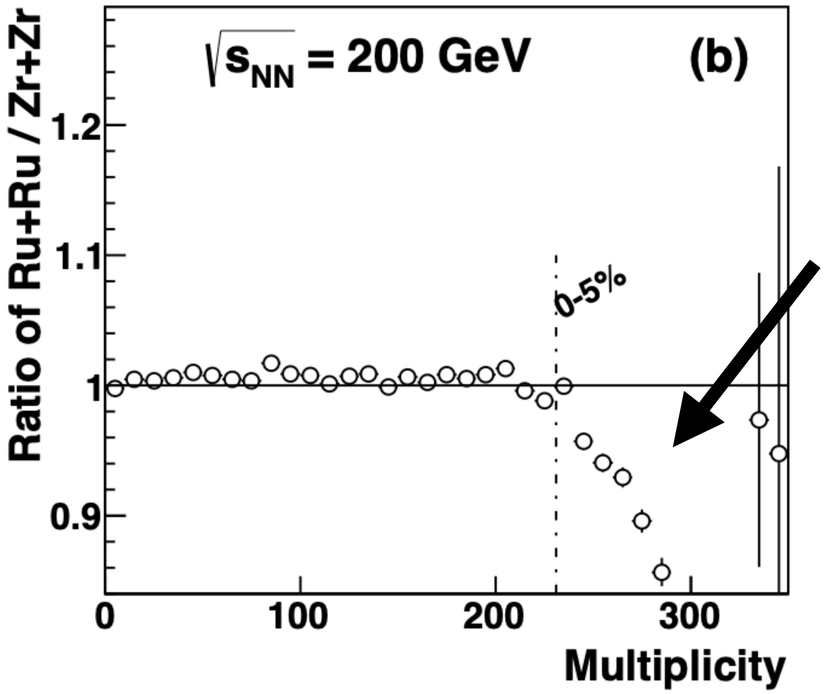

Difference in radius matters

Neutron skin

$$\Delta r_{np} = \langle r_n^2 \rangle^{1/2} - \langle r_p^2 \rangle^{1/2}$$

$$\Delta r_{np}\Big|_{^{96}_{40}\mathrm{Zr}} = 0.12 \pm 0.03 \text{ fm}$$

A. Trzcinska, et al., Phys. Rev. Lett. 87,082501 (2001)

Nucleon in $^{96}_{40}$Zr	R [fm]	a [fm]
p	5.08	0.34
n	5.08	0.46

parameters for case with neutron skin

Hammelmann et al., *Phys.Rev.C* 101 (2020) 6, 061901

halo type

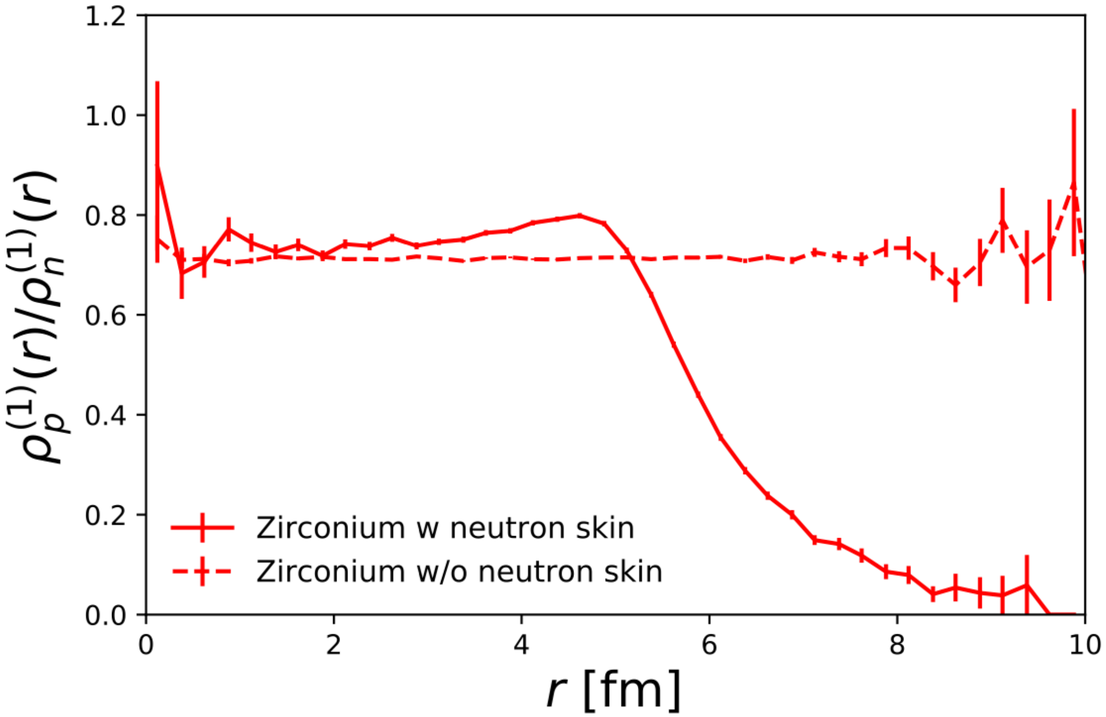

Experimental data is sensitive to details of (spherical) shape

Ru: $R = 5.085\,\text{fm};\ a = 0.46\,\text{fm};\ \beta_2 = 0.053$ (case 2)
Zr: $R = 5.02\,\text{fm};\ a = 0.46\,\text{fm};\ \beta_2 = 0.217$ (case 2)

Deng et al., *Phys.Rev.C* 94 (2016) 041901

Ru: $R = 5.067\,\text{fm};\ a = 0.5\,\text{fm};\ \beta_2 = 0$ (case 3)
Zr: $R = 4.965\,\text{fm};\ a = 0.556\,\text{fm};\ \beta_2 = 0$ (case 3)

Xu et. al., *Phys.Lett.B* 819 (2021) 136453 from DFT then parametrized

Case 3 has a thicker neutron skin in Zr and describes the data best.

R and a affect central events

skin depth a affects peripheral events

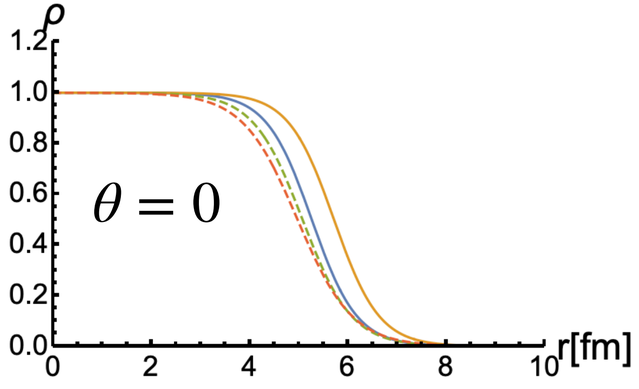

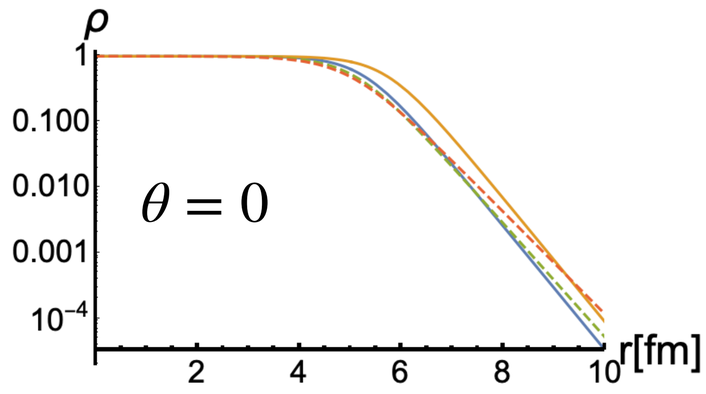

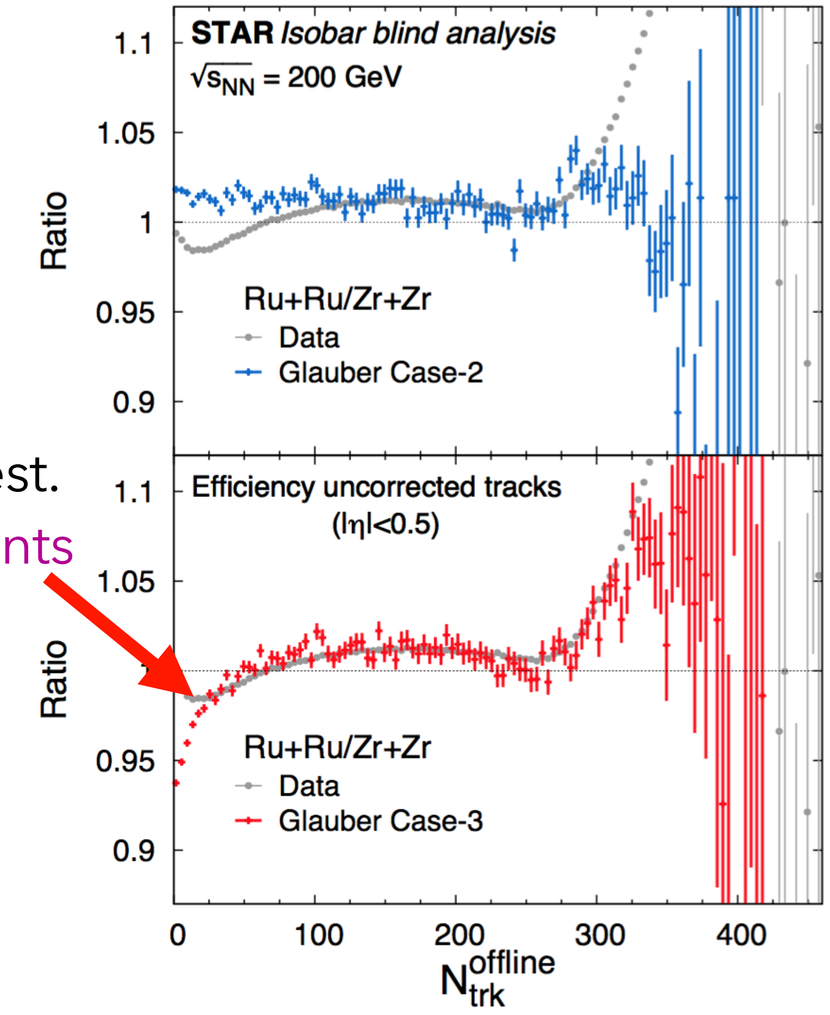

STAR Collaboration, *Phys.Rev.C* 105 (2022) 1, 014901

Effect of deformation: Eccentricity in central collisions

For more elliptic nuclei, the interaction region becomes more elliptic on average for central events, where we have almost complete overlap

Deng et al., *Phys.Rev.C* 94 (2016) 041901

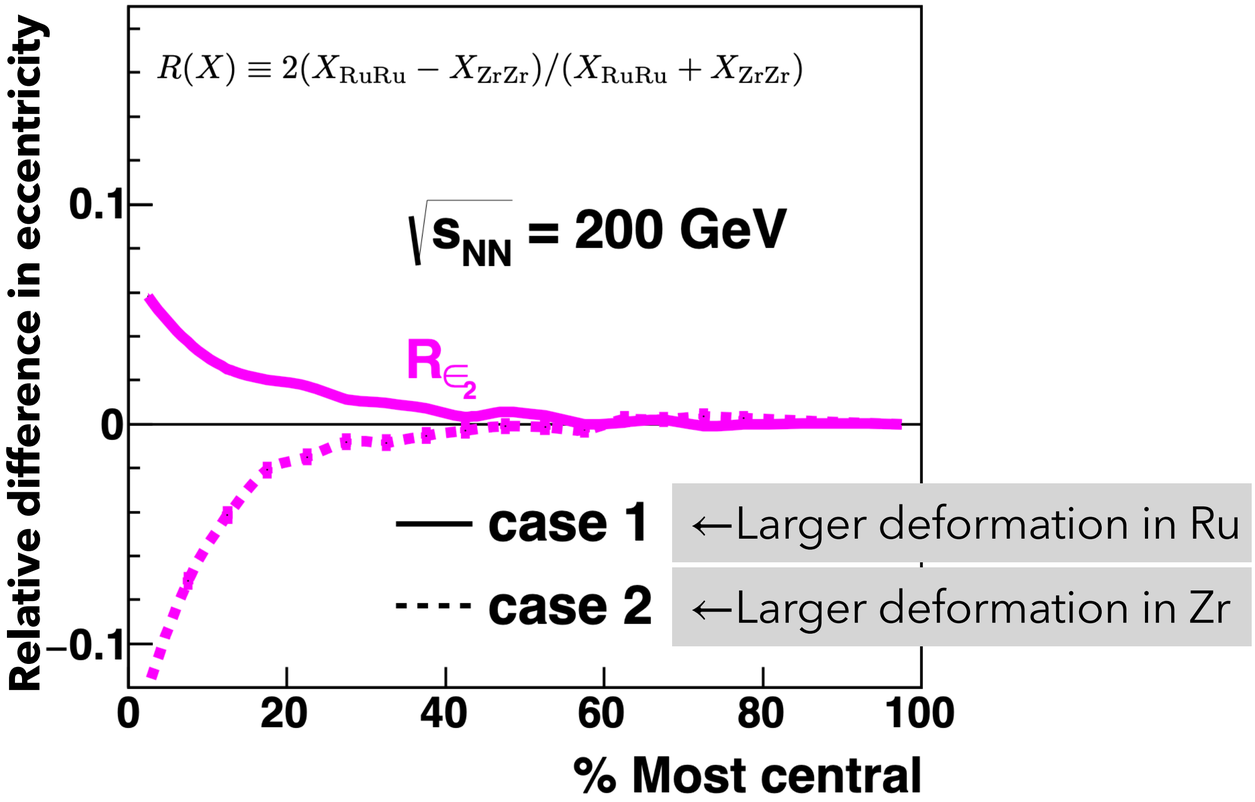

Hammelmann et al., *Phys.Rev.C* 101 (2020) 6, 061901

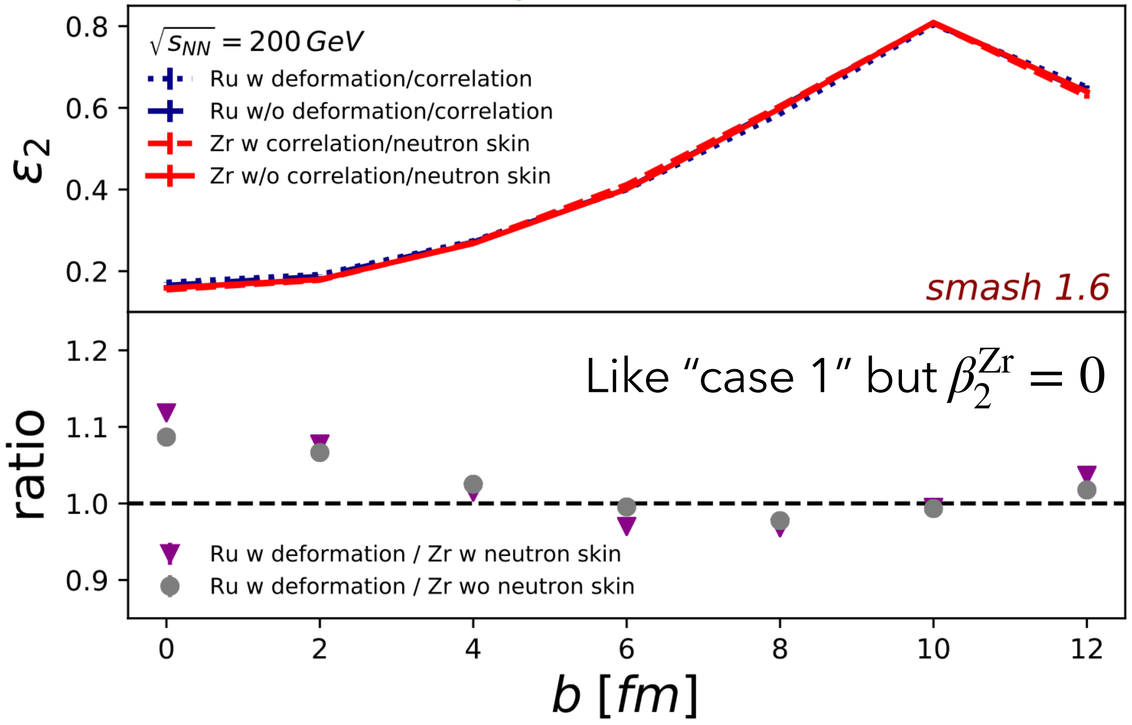

Deformation modifies eccentricity in central collisions
Neutron skin has some weak effect on the anisotropy
also see Xu et al., Phys.Lett.B 819 (2021) 1136453

Improved nuclear density distributions

Compare Woods-Saxon distribution distributions from Density Functional Theory (DFT), using SLy4 mean field including pairing correlations (Hartree-Fock-Bogoliubov (HFB) approach)

Xu et al., Phys. Rev. Lett. 121, 022301 (2018)

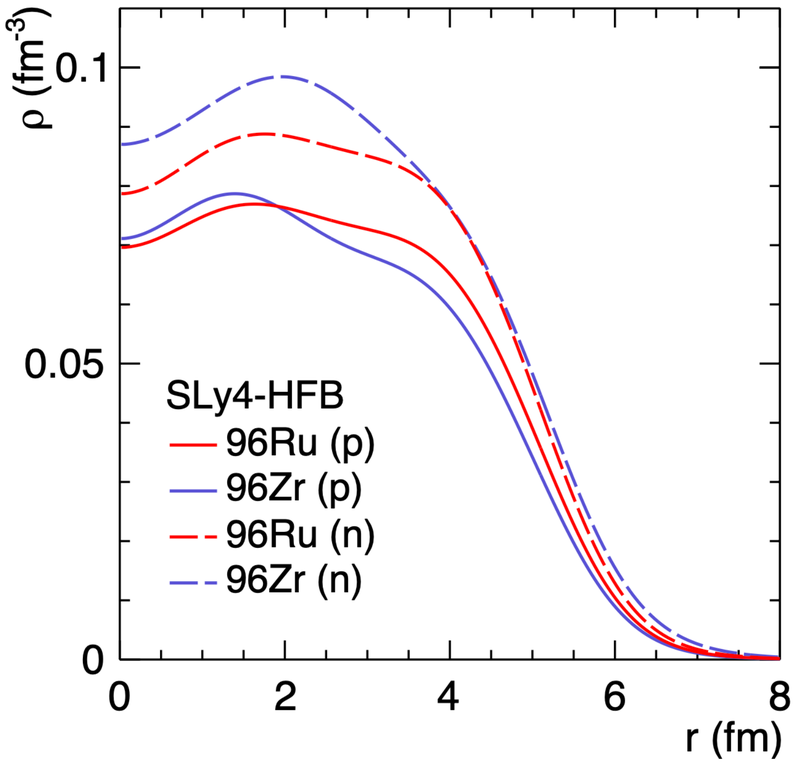

DFT mass radius
Zr: 4.366 fm > Ru: 4.343 fm
opposite to the previous ordering. Changes tail in multiplicity distribution

$$R(X) \equiv 2(X_{\mathrm{RuRu}} - X_{\mathrm{ZrZr}})/(X_{\mathrm{RuRu}} + X_{\mathrm{ZrZr}})$$

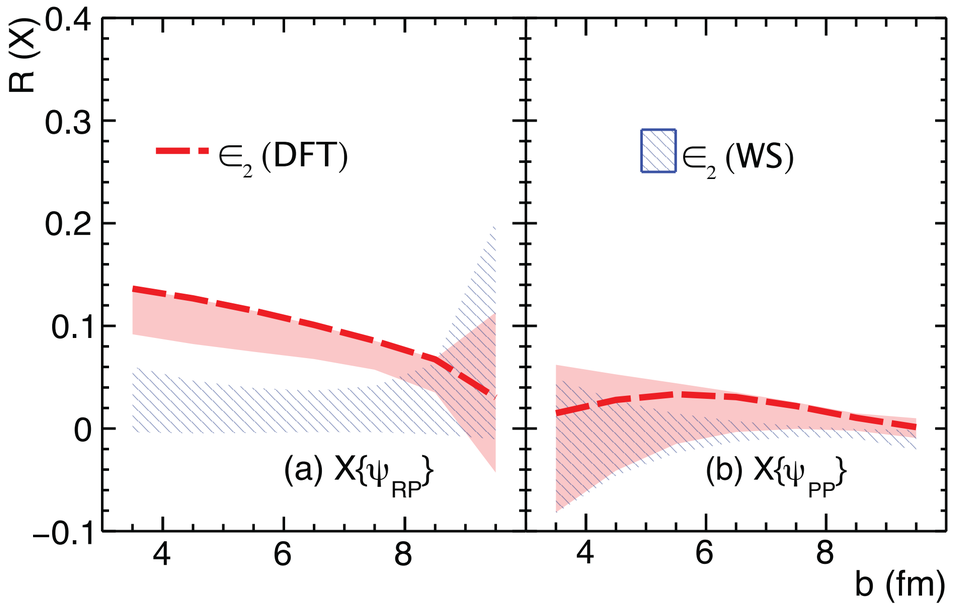

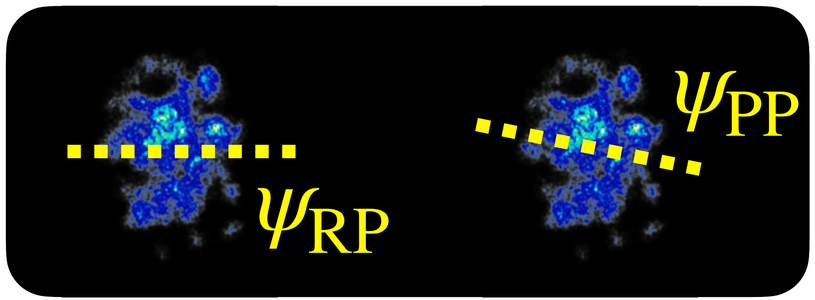

Improved nuclear density distributions

Compare Woods-Saxon distribution distributions from Density Functional Theory (DFT), using SLy4 mean field including pairing correlations (Hartree-Fock-Bogoliubov (HFB) approach)

Xu et al., Phys. Rev. Lett. 121, 022301 (2018)

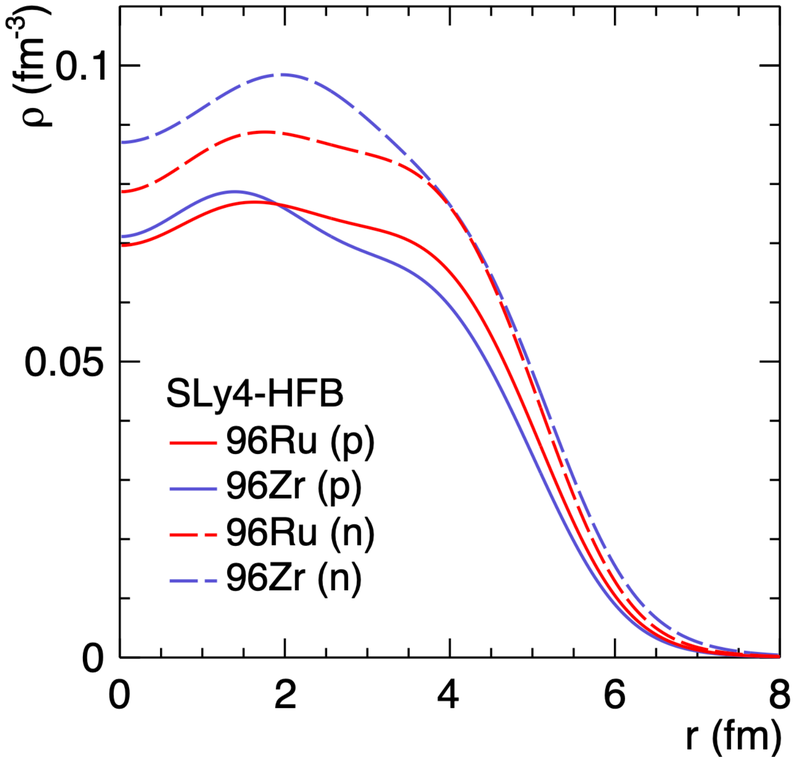

DFT mass radius
Zr: 4.366 fm > Ru: 4.343 fm
opposite to the previous ordering. Changes tail in multiplicity distribution

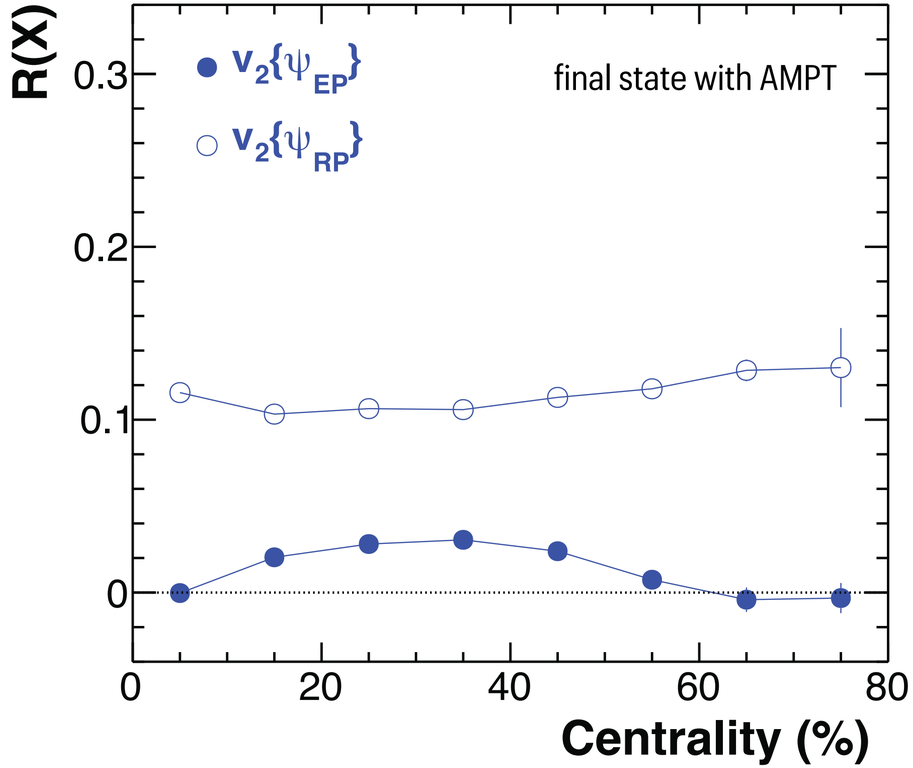

Including octupole deformation β_3

Zhang, Jia, *Phys.Rev.Lett.* 128 (2022) 2, 022301; Nijs, Van der Schee, e-Print: 2112.13771 [nucl-th]

nucleus	R_p [fm]	σ_p [fm]	R_n [fm]	σ_n [fm]	β_2	β_3	σ_{AA} [b]
$^{96}_{44}\mathrm{Ru}(1)$	5.085	0.46	5.085	0.46	0.158	0	4.628
$^{96}_{40}\mathrm{Zr}(1)$	5.02	0.46	5.02	0.46	0.08	0	4.540
$^{96}_{44}\mathrm{Ru}(2)$	5.085	0.46	5.085	0.46	0.053	0	4.605
$^{96}_{40}\mathrm{Zr}(2)$	5.02	0.46	5.02	0.46	0.217	0	4.579
$^{96}_{44}\mathrm{Ru}(3)$	5.06	0.493	5.075	0.505	0	0	4.734
$^{96}_{40}\mathrm{Zr}(3)$	4.915	0.521	5.015	0.574	0	0	4.860
$^{96}_{44}\mathrm{Ru}(4)$	5.053	0.48	5.073	0.49	0.16	0	4.701
$^{96}_{40}\mathrm{Zr}(4)$	4.912	0.508	5.007	0.564	0.16	0	4.829
$^{96}_{44}\mathrm{Ru}(5)$	5.053	0.48	5.073	0.49	0.154	0	4.699
$^{96}_{40}\mathrm{Zr}(5)$	4.912	0.508	5.007	0.564	0.062	0.202	4.871

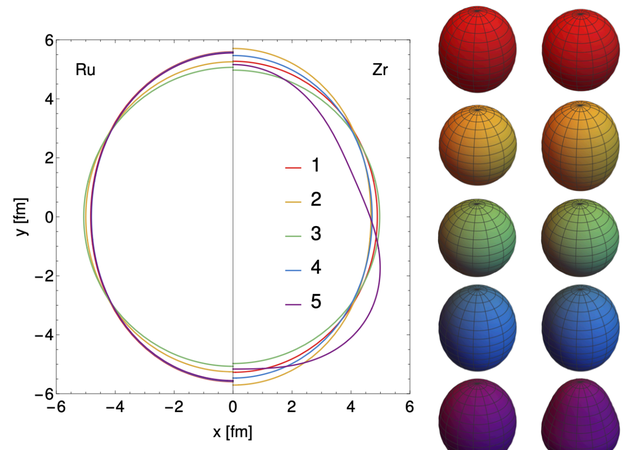

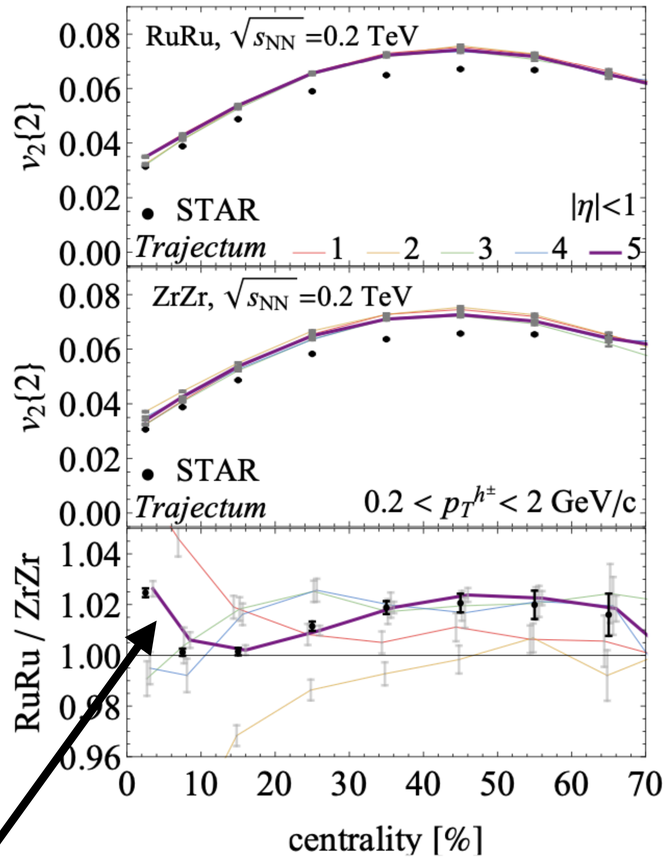

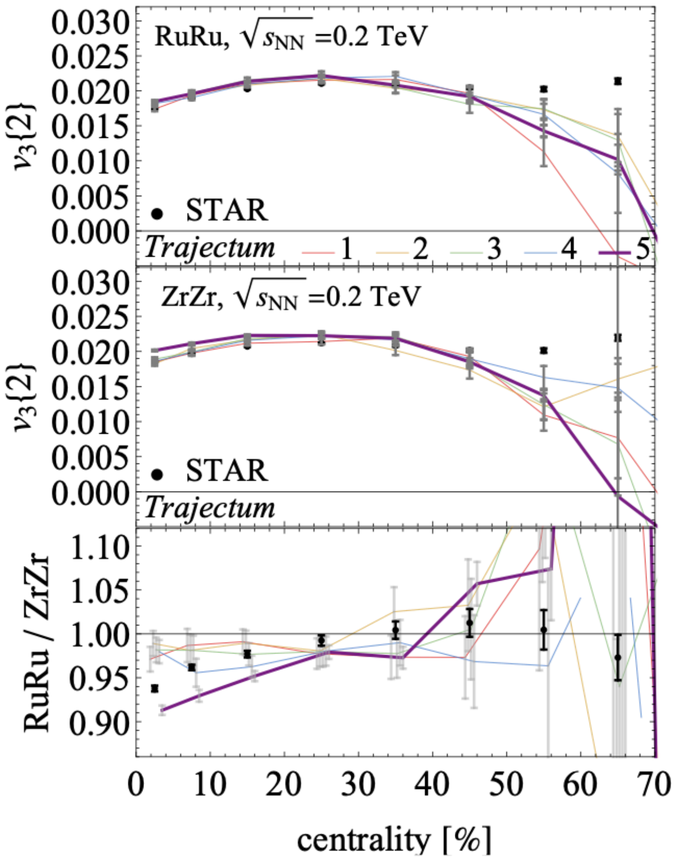

The Hybrid Framework

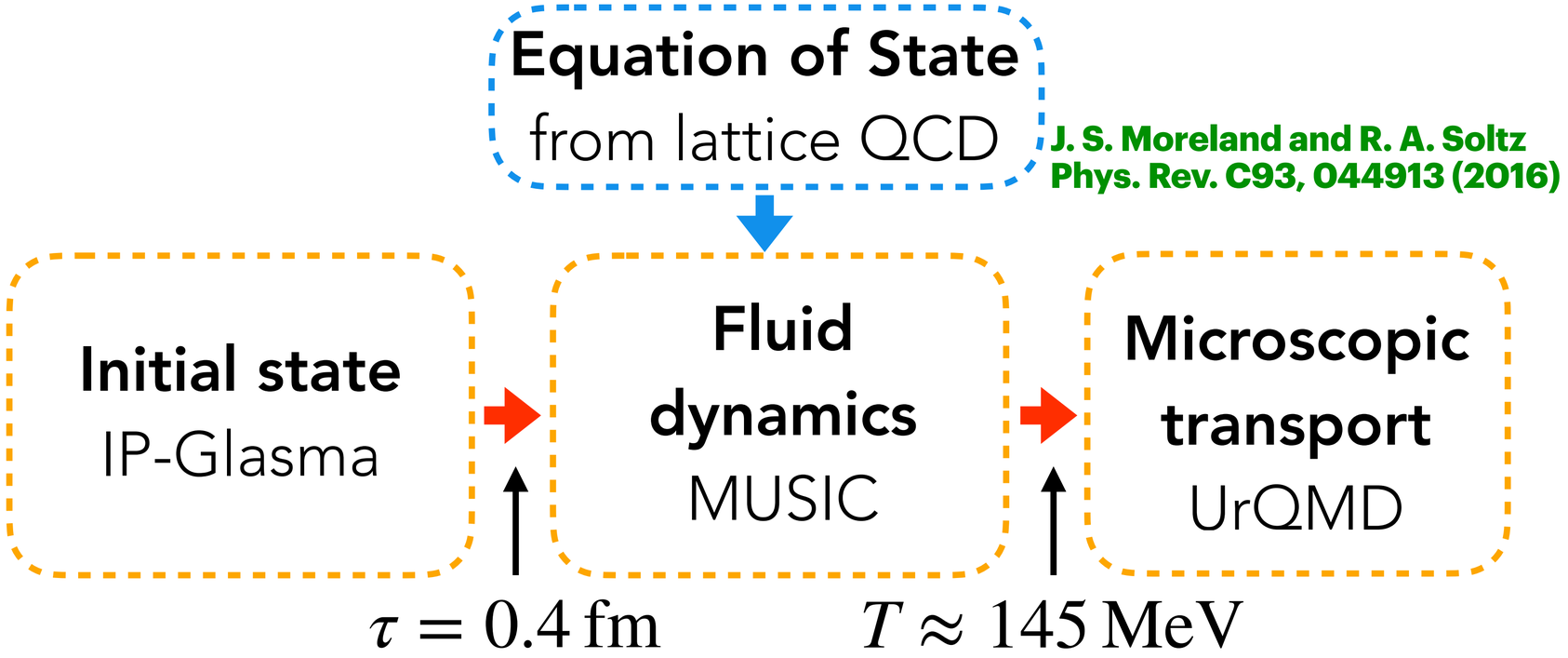

Described in detail in

B. Schenke, C. Shen, P. Tribedy, Phys. Rev. C 102 (2020) 4, 044905

"Running the gamut of high energy nuclear collisions"

The term gamut was adopted from the field of **music**, where in middle age Latin "gamut" meant the entire range of musical notes of which musical melodies are composed

- **Exactly match $T^{\mu\nu}$ when switching from one part to the next**

B. Schenke, P. Tribedy, and R. Venugopalan, Phys. Rev. Lett. 108, 252301 (2012)
B. Schenke, S. Jeon, and C. Gale, Phys. Rev. Lett. 106, 042301 (2011)
S. A. Bass et al., Prog. Part. Nucl. Phys. 41, 255 (1998); M. Bleicher et al., J. Phys. G25, 1859 (1999)

INITIAL STATE

B. Schenke, P. Tribedy, and R. Venugopalan, Phys. Rev. Lett. 108, 252301 (2012)

In IP-Glasma sample nucleon positions from nuclear density distribution.
Then project on the plane transverse to the beam line.

We assumed a 2D Gaussian density distribution for every nucleon: $\frac{1}{2\pi w^2} e^{-\frac{x^2+y^2}{2w^2}}$

We use a width $w = 0.4\,\mathrm{fm}$ **(and include subnucleon hot spots with width** $w_q = 0.11\,\mathrm{fm}$**)**

(constrained by diffractive data from e+p collisions at HERA)

Sum over the hot spots leads to a distribution that determines the saturation scale $Q_s(\vec{x}_\perp)$

Then sample color charges from local Gaussian distribution with variance $\propto Q_s^2(\vec{x}_\perp)$

These moving charges make color current in Yang Mills equations. Solve Yang-Mills equations with two 'colliding' currents → Initial energy momentum tensor

Full hydro: Zr and Ru compared to other systems

Schenke, Shen, Tribedy, *Phys.Rev.C* 102 (2020) 4, 044905

IP-Glasma+MUSIC+UrQMD

Nucleus	R [fm]	a [fm]	β_2	β_4
^{238}U	6.81	0.55	0.28	0.093
^{208}Pb	6.62	0.546	0	0
^{197}Au	6.37	0.535	-0.13	-0.03
^{129}Xe	5.42	0.57	0.162	-0.003
^{96}Ru	5.085	0.46	0.158	0
^{96}Zr	5.02	0.46	0	0

$\eta/s = 0.12$

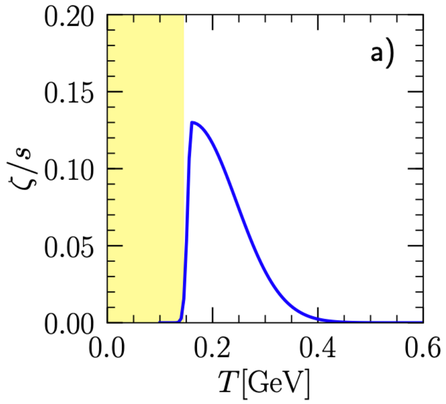

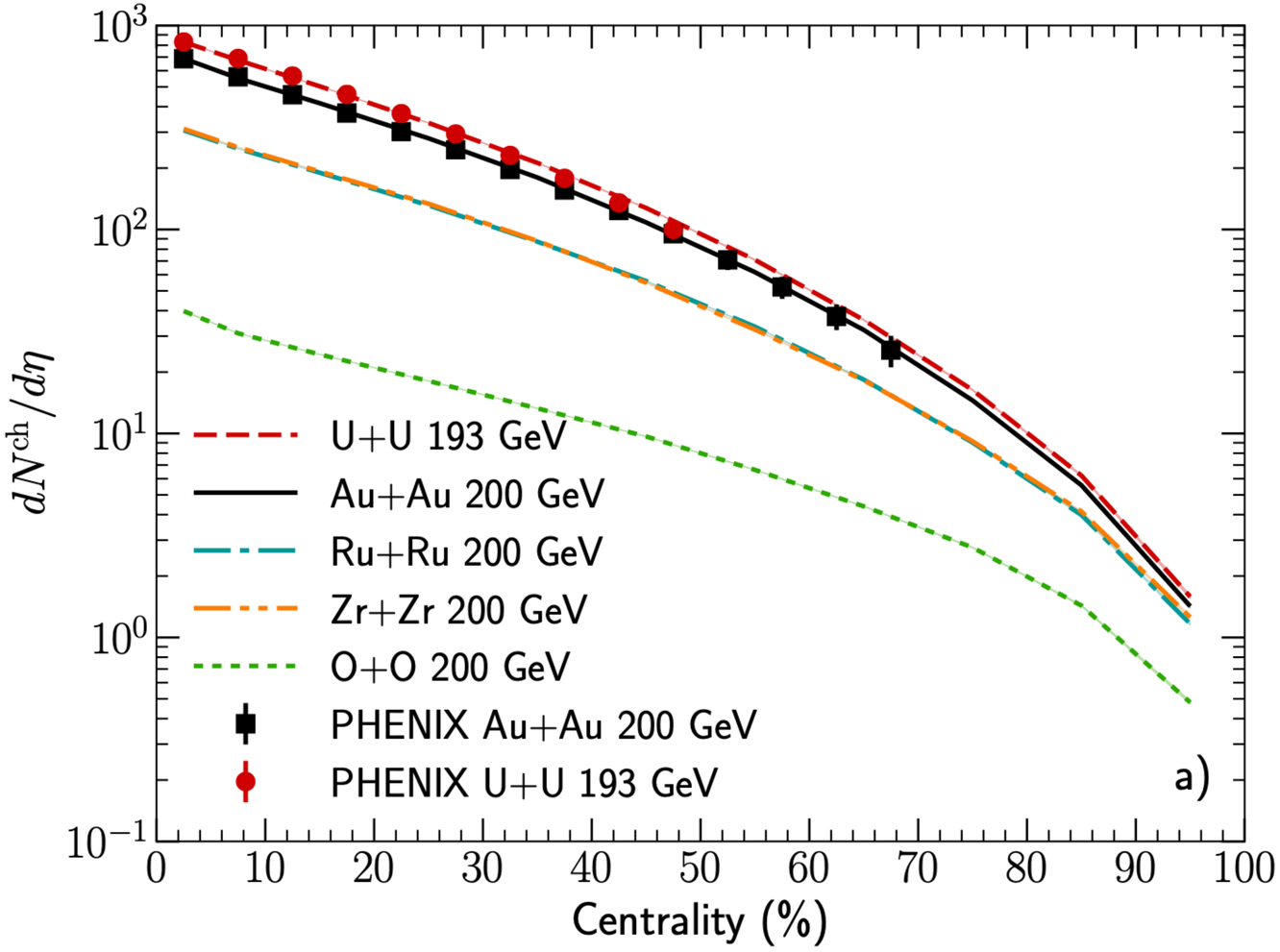

Mean transverse momentum

Schenke, Shen, Tribedy, *Phys.Rev.C* 102 (2020) 4, 044905

IP-Glasma+MUSIC+UrQMD

Nucleus	R [fm]	a [fm]	β_2	β_4
^{238}U	6.81	0.55	0.28	0.093
^{208}Pb	6.62	0.546	0	0
^{197}Au	6.37	0.535	-0.13	-0.03
^{129}Xe	5.42	0.57	0.162	-0.003
^{96}Ru	5.085	0.46	0.158	0
^{96}Zr	5.02	0.46	0	0

$\eta/s = 0.12$

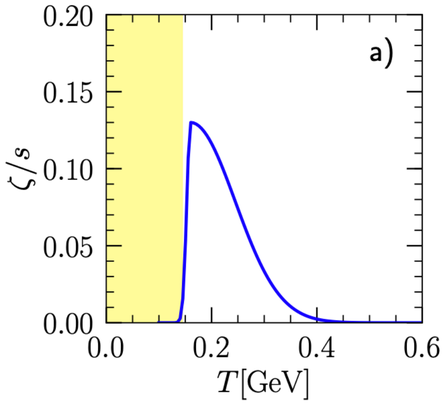

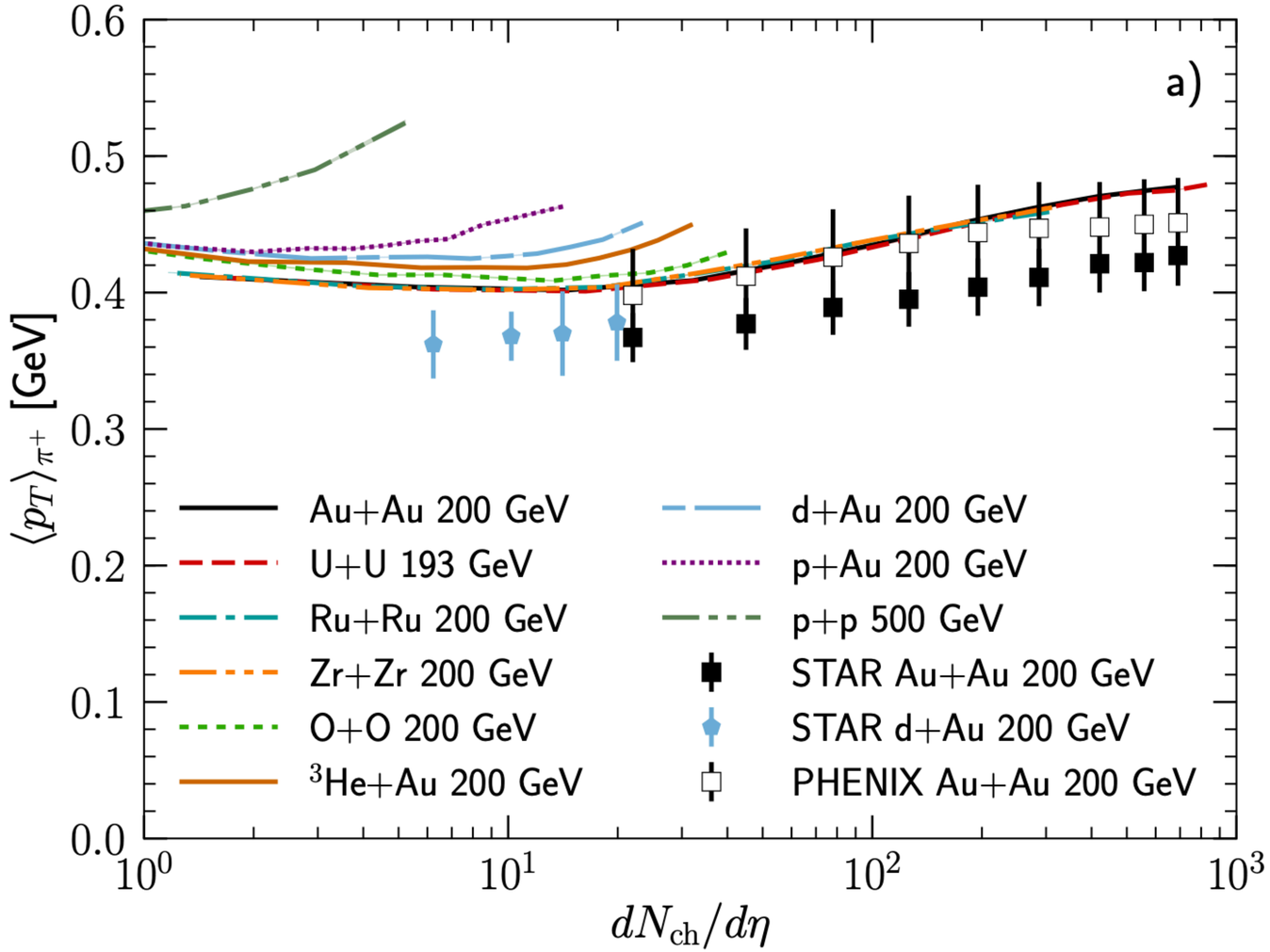

Anisotropic flow

Schenke, Shen, Tribedy, *Phys.Rev.C* 102 (2020) 4, 044905

Nucleus	R [fm]	a [fm]	β_2	β_4
^{238}U	6.81	0.55	0.28	0.093
^{208}Pb	6.62	0.546	0	0
^{197}Au	6.37	0.535	-0.13	-0.03
^{129}Xe	5.42	0.57	0.162	-0.003
^{96}Ru	5.085	0.46	0.158	0
^{96}Zr	5.02	0.46	0	0

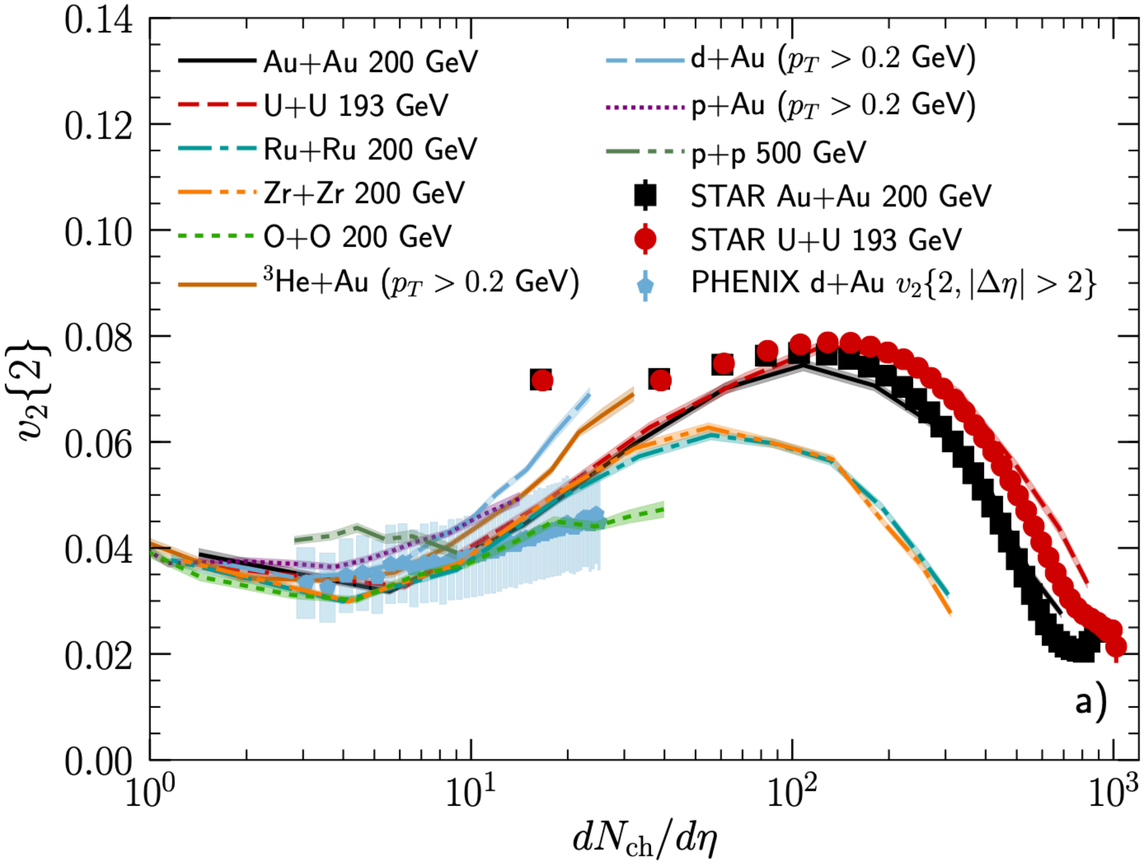

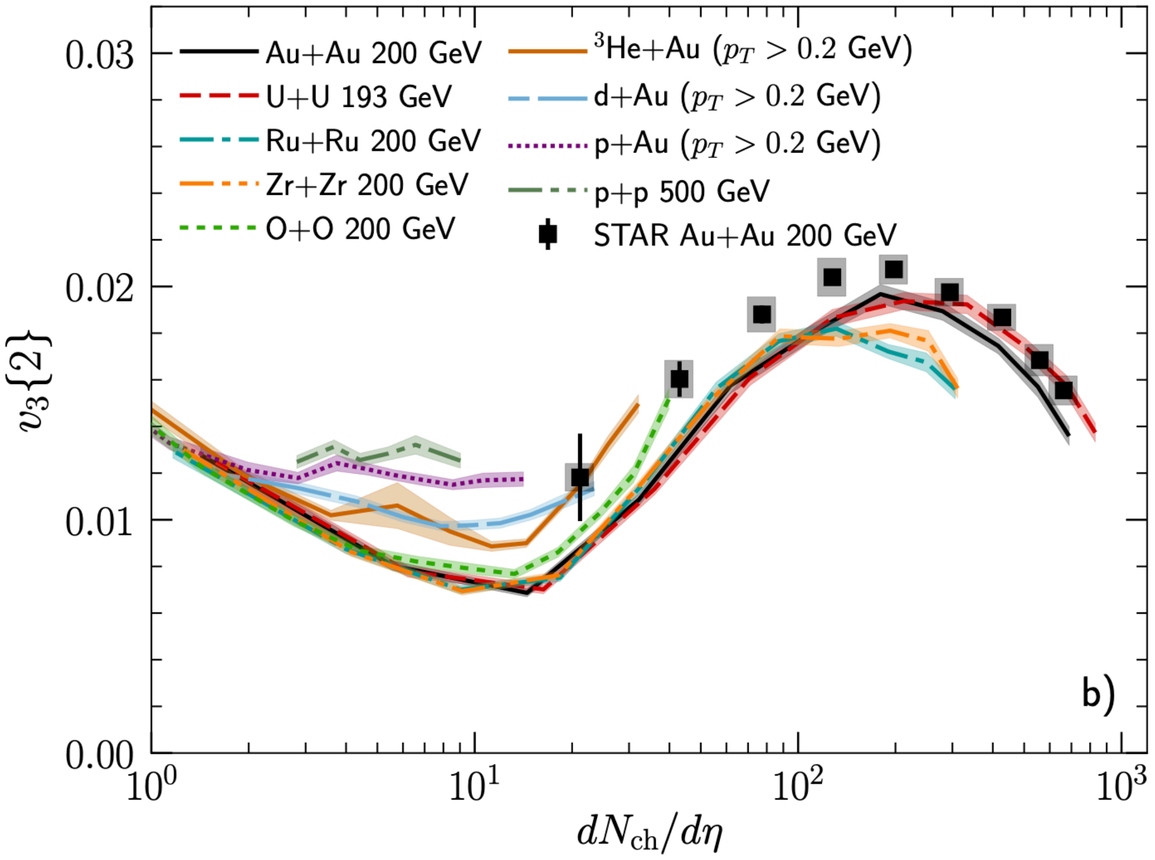

Effects of medium properties

Mean transverse momentum **Xu et al., e-Print: 2111.14812 [nucl-th]**

$\langle p_T \rangle$

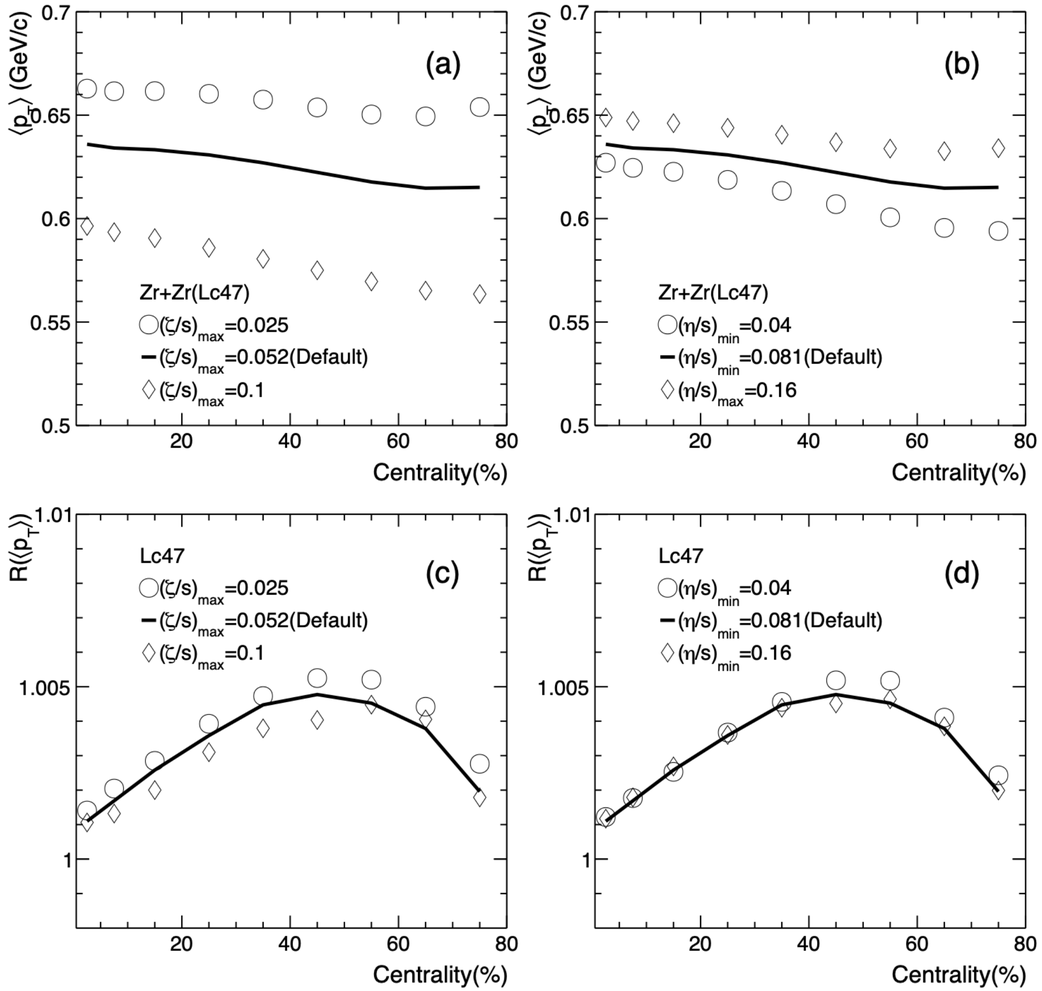

$$R_{\langle p_\perp \rangle} = \frac{\langle p_\perp \rangle^{\mathrm{Ru+Ru}}}{\langle p_\perp \rangle^{\mathrm{Zr+Zr}}}$$

using TRENTO initial state

Bernhard, Moreland, Bass, Liu, Heinz
Phys. Rev. C 94, 024907 (2016)

iEBE-VISHNU hydro

Shen, Qiu, Song, Bernhard, Bass, Heinz
Comput. Phys. Commun. 199, 61 (2016)

Ratio has weak sensitivity to medium parameters/evolution

Hydrodynamic calculation using WS and charge dependent observables

Schenke, Shen, Tribedy, *Phys.Rev.C* 99 (2019) 4, 044908

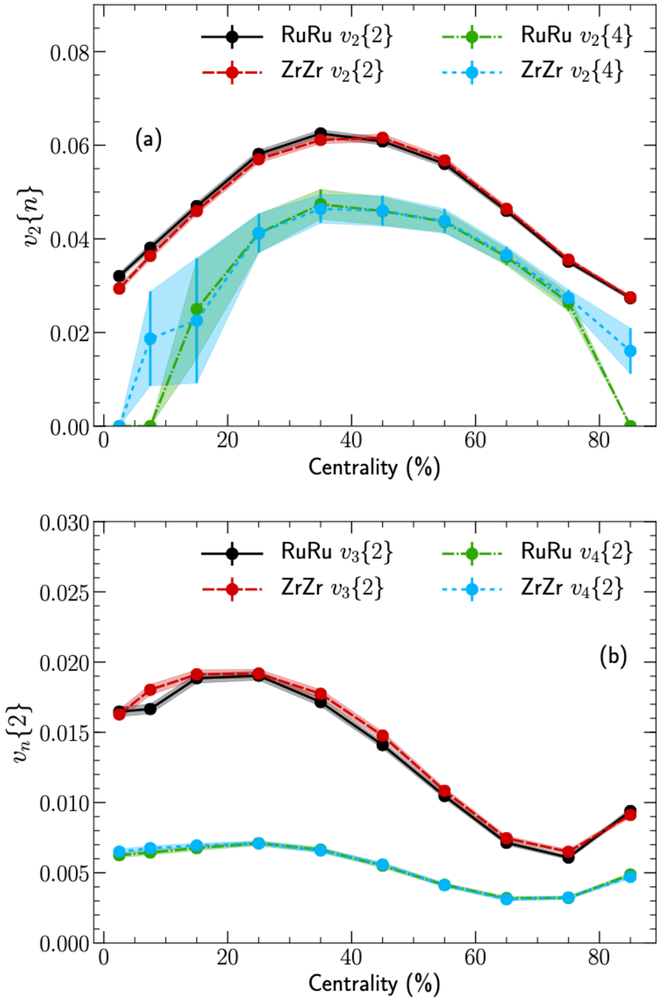

$$\Delta C_{mnk} = C_{mnk}(\mathrm{OS}) - C_{mnk}(\mathrm{SS})$$

$$C_{mnk}(\mathrm{OS}) = \langle \cos(m\phi_\alpha^{\pm} + n\phi_\beta^{\mp} - k\phi_c) \rangle$$

$$C_{mnk}(\mathrm{SS}) = \langle \cos(m\phi_\alpha^{\pm} + n\phi_\beta^{\pm} - k\phi_c) \rangle$$

Nucleus	R [fm]	a [fm]	β_2	β_4
^{96}Ru	5.085	0.46	0.158	0
^{96}Zr	5.02	0.46	0	0

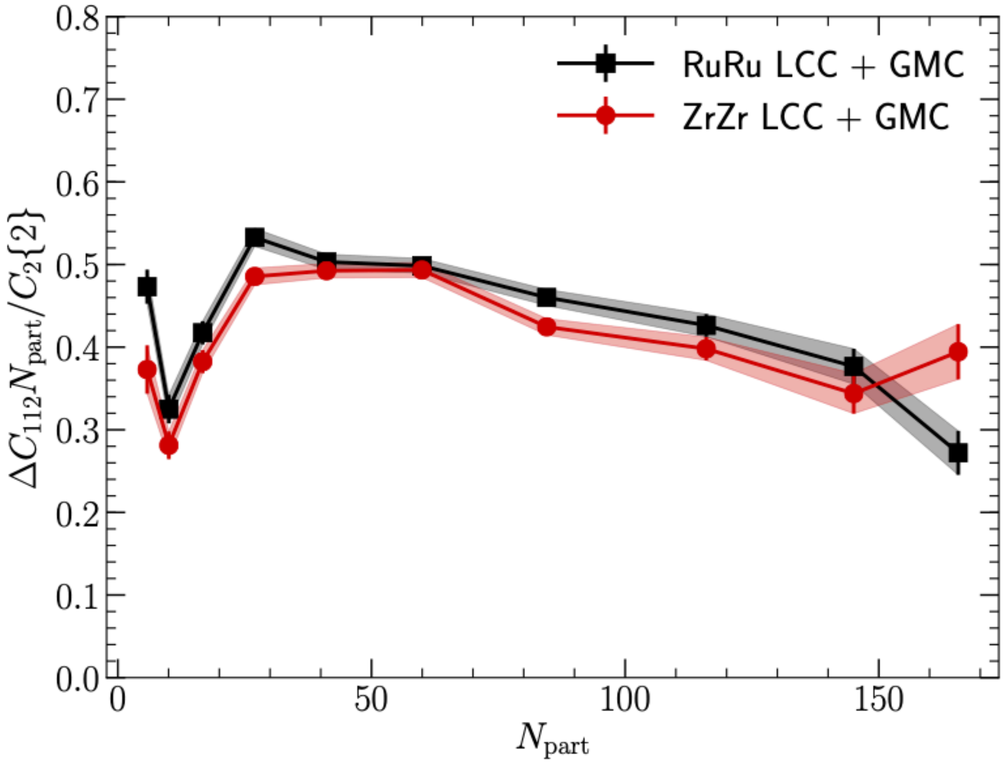

Comparison to STAR data

STAR Collaboration, *Phys.Rev.C* 105 (2022) 1, 014901

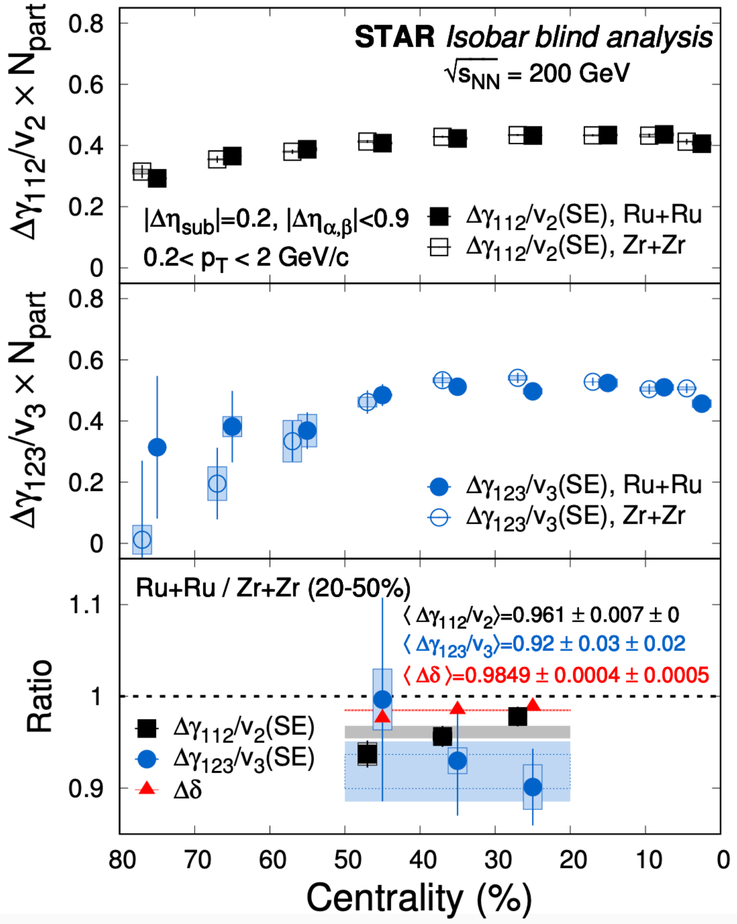

$$\Delta C_{mnk} = C_{mnk}(\mathrm{OS}) - C_{mnk}(\mathrm{SS})$$

$$C_{mnk}(\mathrm{OS}) = \langle \cos(m\phi_\alpha^{\pm} + n\phi_\beta^{\mp} - k\phi_c) \rangle$$

$$C_{mnk}(\mathrm{SS}) = \langle \cos(m\phi_\alpha^{\pm} + n\phi_\beta^{\pm} - k\phi_c) \rangle$$

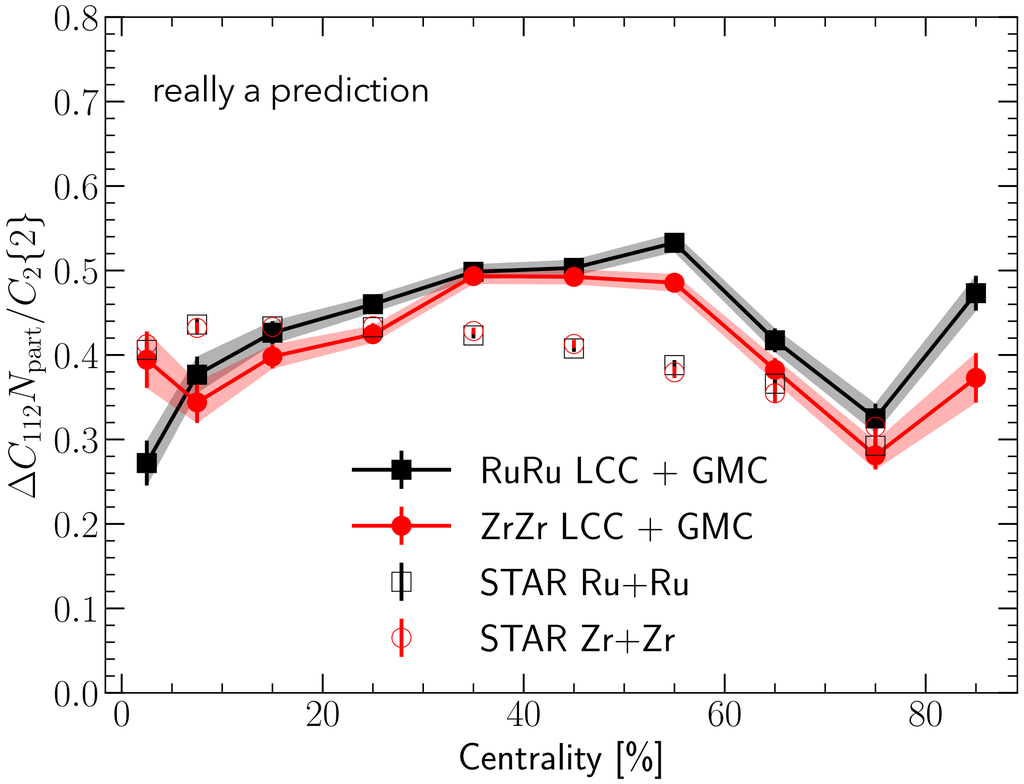

Schenke, Shen, Tribedy, *Phys.Rev.C* 99 (2019) 4, 044908

Summary

- Hydrodynamics converts spatial geometry of the interaction region into observable features of the particle distributions
- Details of nuclear density distribution affect the deposited energy
- Precision heavy ion data is sensitive to the details of the nuclear structure - e.g. can tell the difference between isobars
- Hydrodynamic calculations can predict these differences, sensitive to e.g. different types and degrees of deformation and neutron skin
- Effects of medium properties can be reduced by choosing proper observables
- For charge dependent quantities precision calculations get harder: Must control shape as well as conservation laws

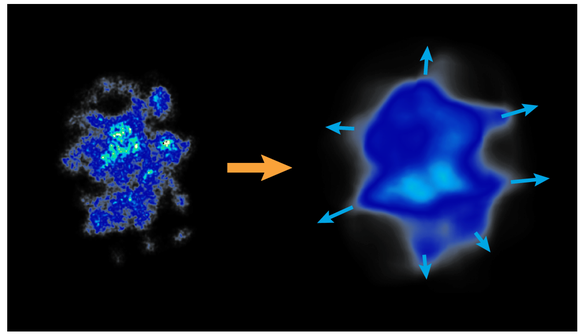

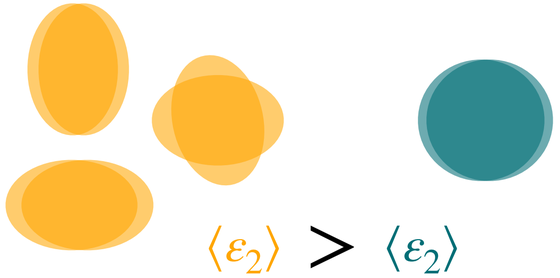

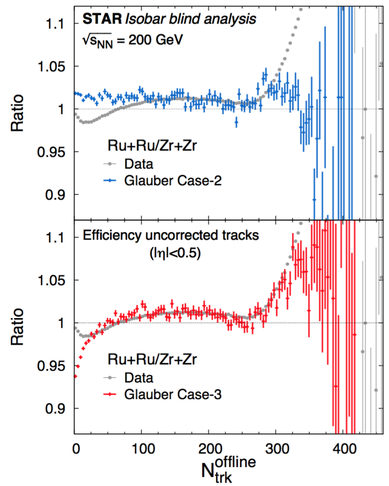

BACKUP

MUSIC → UrQMD

Sample particles on the freeze-out surface
(surface of constant energy density)
according to

$$E\frac{dN_i}{d^3p} = \frac{g_i}{(2\pi)^3}\Delta^3\Sigma_\mu p^\mu (f_i^{(0)} + \delta f_i)$$

then feed particles into UrQMD

S. A. Bass et al., Prog. Part. Nucl. Phys. 41, 255–369 (1998)
M. Bleicher et al., J. Phys. G25, 1859–1896 (1999)

which performs resonance decays and scattering
according to hadronic cross sections

Exact conservation laws should be fulfilled when converting to pa

Local charge conservation

Implement simple model that respects local charge conservation

- For each sampled particle sample its anti-particle in the same surface cell P. Bozek, W. Broniowski, PRL 109 062301 (2012)
- The common boost will introduce a correlation between the two opposite sign particles in momentum space

local rest frame

boost with fluid velocity

Implemented in sampler iSS available at: https://github.com/chunshen1987/iSS

Global momentum conservation

- Ideally implement local momentum conservation
- But it is not trivial and left for future work
- We will concentrate on observables where the effect of local momentum conservation cancels
- For now: global momentum conservation
  - Compute net momentum of the system $\langle \vec{p} \rangle = \sum_i \vec{p}_i$
  - Then we correct every particle's momentum by

$$\vec{p}_i' = \vec{p}_i - \frac{p_{T,i}^2}{\langle p_T^2 \rangle} \langle \vec{p} \rangle$$

  - Correction to each particle's momentum is order *1/N* where *N* is the total number of particles in the sampled event

Implemented in sampler iSS available at: `https://github.com/chunshen1987/iSS`

Power spectrum of momentum anisotropies

v_n as a function of n in central Pb+Pb collisions

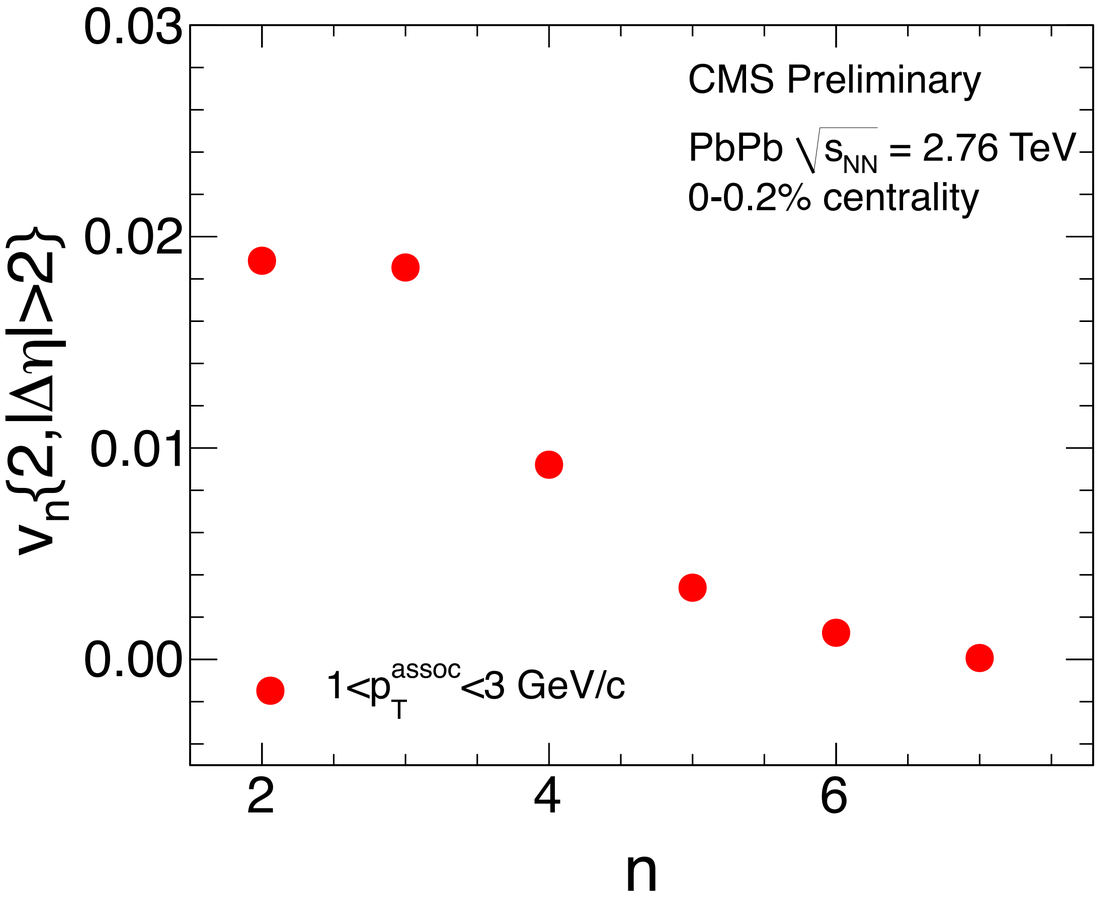

CMS Collaboration, JHEP 02 (2014) 088

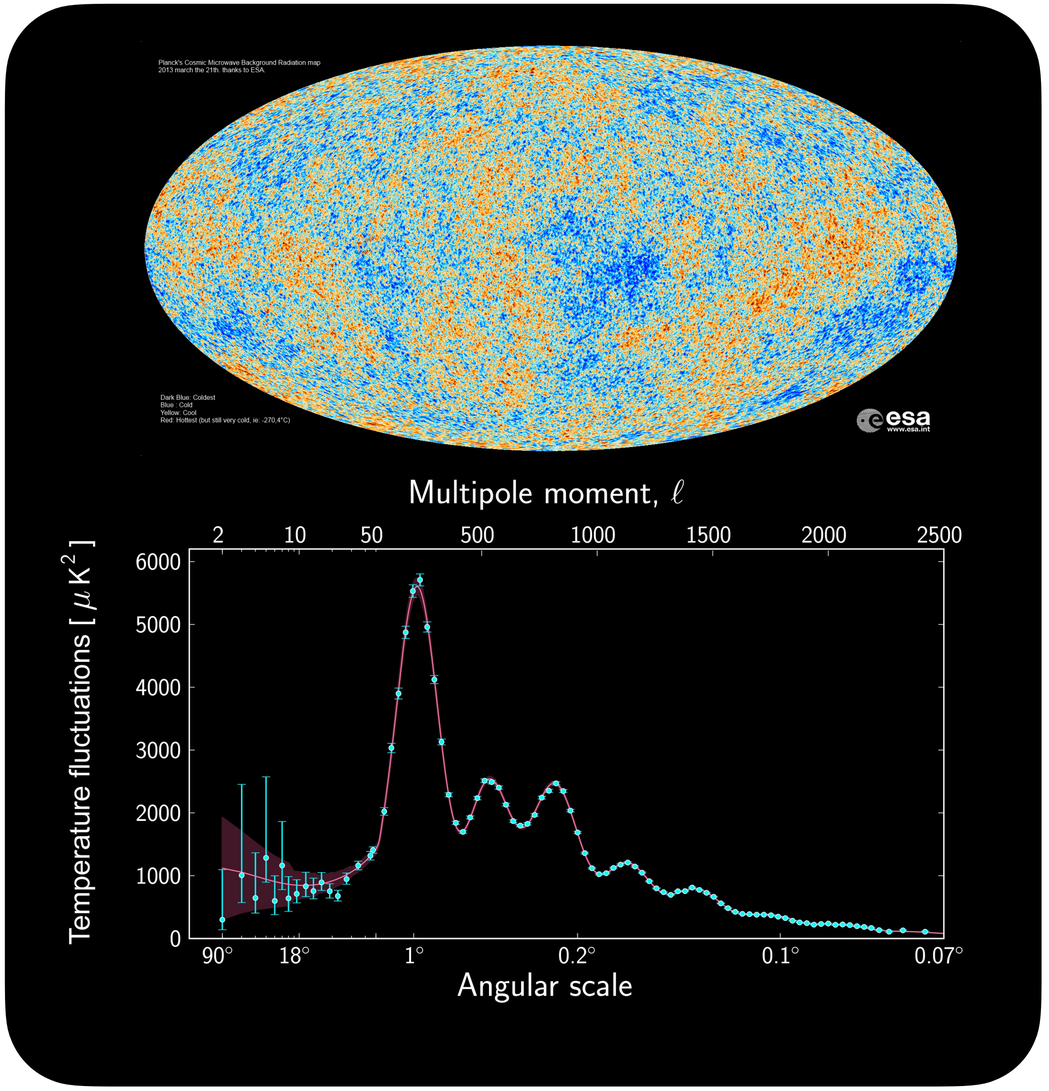

PLANCK Coll. A&A 571, A16 (2014)

Mean transverse momentum

Sensitivity to nuclear deformation **Xu et al., e-Print: 2111.14812 [nucl-th]**

$$R_{\langle p_\perp \rangle} = \frac{\langle p_\perp \rangle^{\mathrm{Ru+Ru}}}{\langle p_\perp \rangle^{\mathrm{Zr+Zr}}}$$

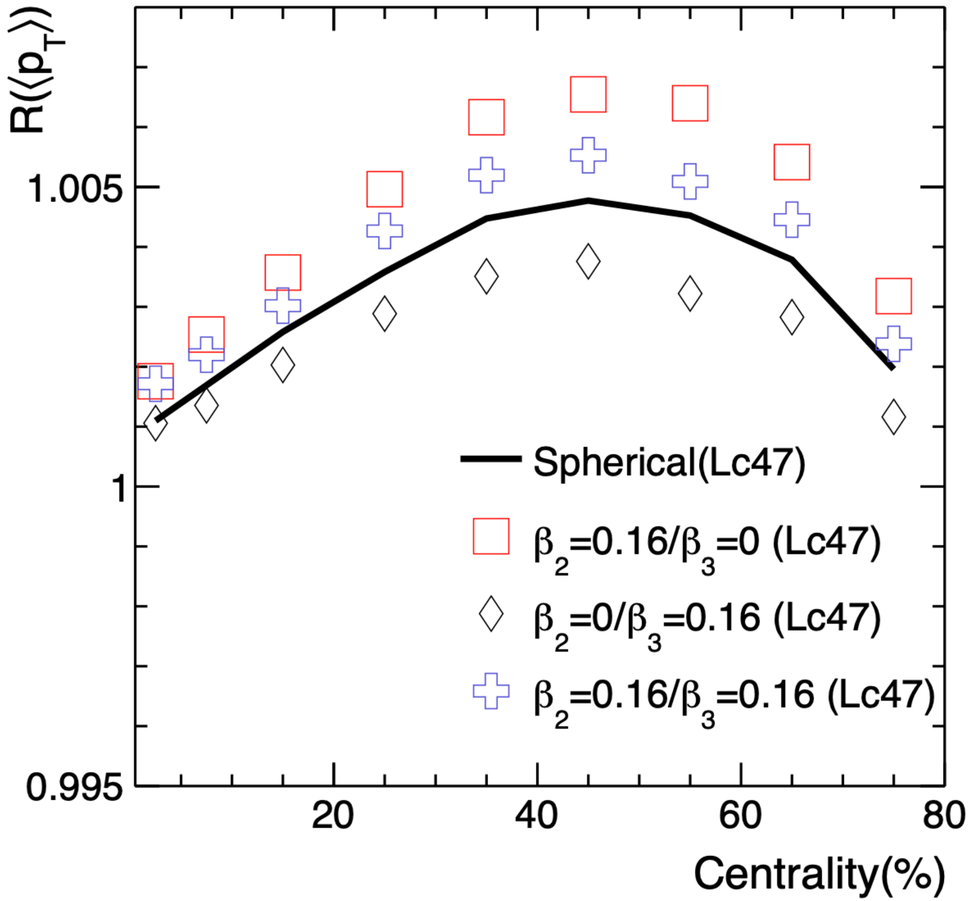

Deformation effectively reduces overlap area

$$S_T = \pi \langle r_T^2 \rangle \sqrt{1 - \varepsilon_2^2}$$

Mean transverse momentum

$\langle p_T \rangle$ correlation with v_2 **Xu et al., e-Print: 2111.14812 [nucl-th]**

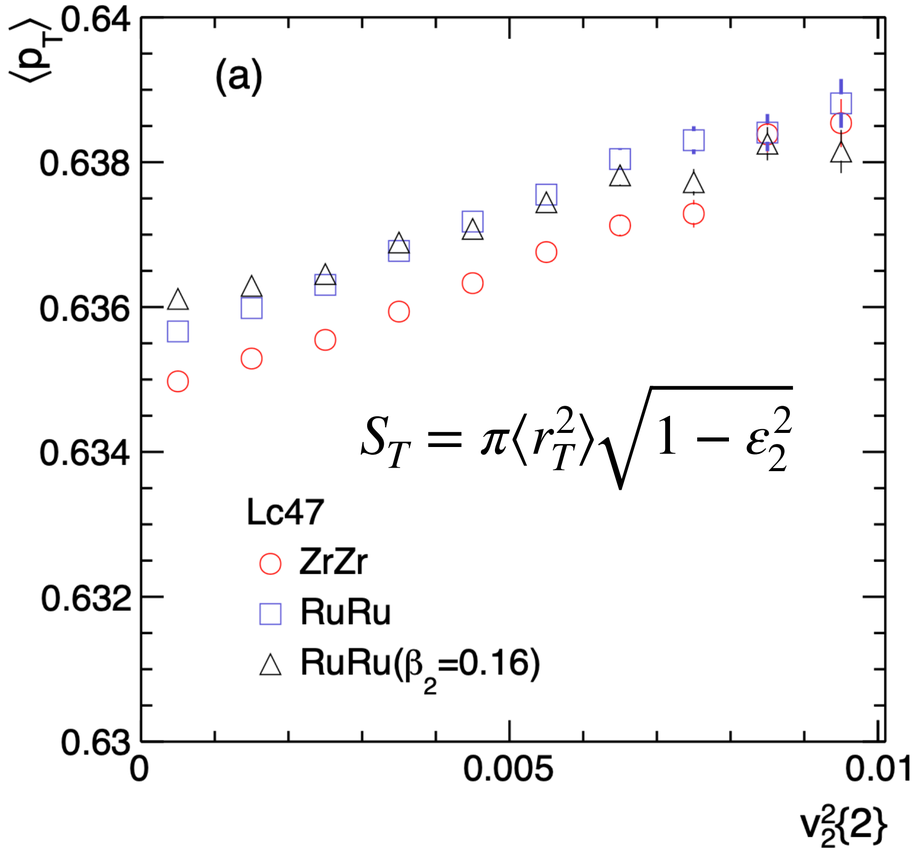

ε_2 fluctuations dominate

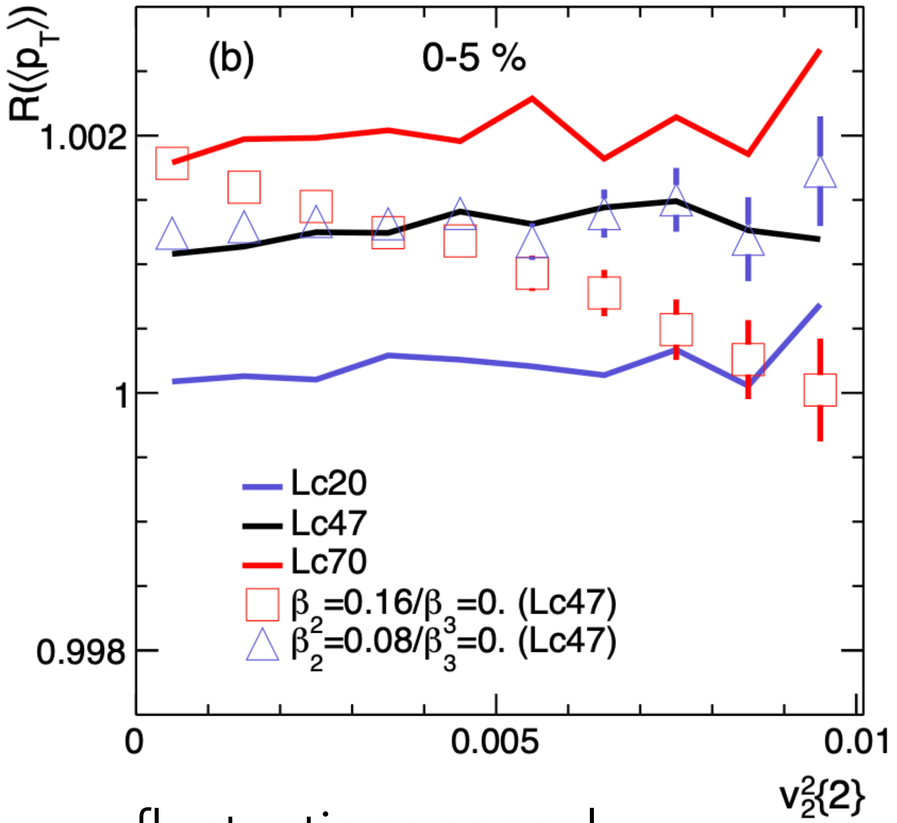

fluctuations cancel, anti-correlation from deformation survives

Mean transverse momentum

and its sensitivity to neutron skin and deformation **Xu et al., e-Print: 2111.14812 [nucl-th]**

Nuclear densities from DFT but parametrized using the WS expression with

	^{96}Ru				^{96}Zr			
	ρ_0	R	a	β_2	ρ_0	R	a	β_3
Lc20	0.161	5.076	0.483	0.00	0.166	4.994	0.528	0.00
Lc47	0.159	5.093	0.488	0.00	0.163	5.022	0.538	0.00
Lc70	0.157	5.114	0.487	0.00	0.160	5.045	0.543	0.00
Lc47Def	0.159	5.090	0.473	0.16	0.163	5.016	0.527	0.16

The $\langle p_T \rangle$ is sensitive to the neutron skin and deformation because

$$\langle p_T \rangle \sim \sqrt{N_{\text{part}}/S_T}$$ where the transverse area $S_T = \pi \langle r_T^2 \rangle \sqrt{1-\varepsilon_2^2}$ (ellipse)

and the neutron skin affects $\langle r_T^2 \rangle$ and deformation affects ε_2

Mean transverse momentum

Sensitivity to nuclear density distribution (spherical case) **Xu et al., e-Print: 2111.14812 [nucl-th]**

$\langle p_T \rangle$

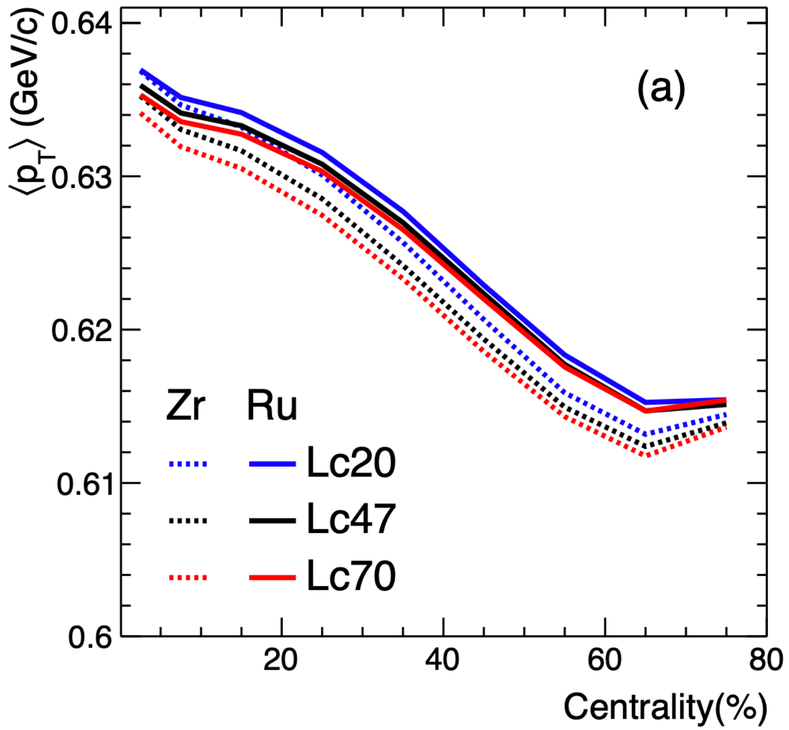

	^{96}Ru				^{96}Zr			
	ρ_0	R	a	β_2	ρ_0	R	a	β_3
Lc20	0.161	5.076	0.483	0.00	0.166	4.994	0.528	0.00
Lc47	0.159	5.093	0.488	0.00	0.163	5.022	0.538	0.00
Lc70	0.157	5.114	0.487	0.00	0.160	5.045	0.543	0.00

Smaller size, larger $\langle p_T \rangle$